AD-A097 642 TRW DEFENSE AND SPACE SYSTEMS GROUP REDONDO BEACH CA F/G 19/4
EVALUATION OF AN UPSTREAM-INDUCED GROUND MOTION WAVEFORM PREDIC--ETC(U)
MAR 80 G M TERAOKA, N LIPNER DNA001-79-C-0401

UNCLASSIFIED DNA-5237F NL

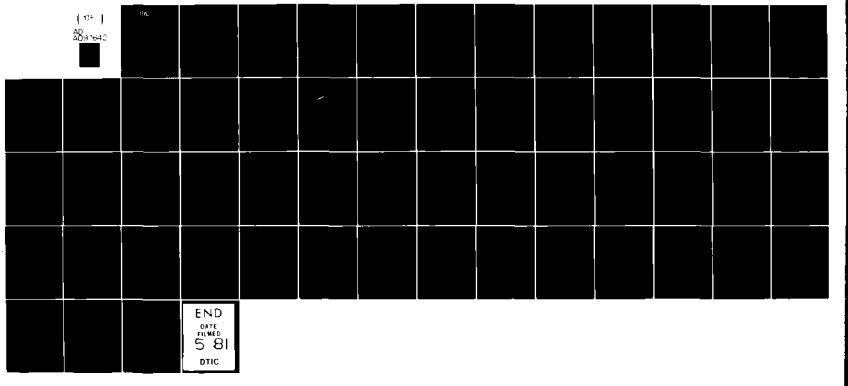

LEVEL II

DNA 5237F

EVALUATION OF AN UPSTREAM-INDUCED GROUND MOTION WAVEFORM PREDICTION PROCEDURE

G. M. Teraoka
N. Lipner
TRW Defense and Space Systems Group
One Space Park
Redondo Beach, California 90278

15 March 1980

Final Report for Period 25 June 1979—15 March 1980

CONTRACT No. DNA 001-79-C-0401

APPROVED FOR PUBLIC RELEASE;
DISTRIBUTION UNLIMITED.

THIS WORK SPONSORED BY THE DEFENSE NUCLEAR AGENCY
UNDER RDT&E RMSS CODE B344079462 H53BAXSX37720 H2590D.

Prepared for
Director
DEFENSE NUCLEAR AGENCY
Washington, D. C. 20305

Destroy this report when it is no longer needed. Do not return to sender.

PLEASE NOTIFY THE DEFENSE NUCLEAR AGENCY, ATTN: STTI, WASHINGTON, D.C. 20305, IF YOUR ADDRESS IS INCORRECT, IF YOU WISH TO BE DELETED FROM THE DISTRIBUTION LIST, OR IF THE ADDRESSEE IS NO LONGER EMPLOYED BY YOUR ORGANIZATION.

UNCLASSIFIED

SECURITY CLASSIFICATION OF THIS PAGE (When Data Entered)

REPORT DOCUMENTATION PAGE	READ INSTRUCTIONS BEFORE COMPLETING FORM
1. REPORT NUMBER: DNA 5237F	2. GOVT ACCESSION NO.: AD-A097642	3. RECIPIENT'S CATALOG NUMBER:
4. TITLE (and Subtitle): EVALUATION OF AN UPSTREAM-INDUCED GROUND MOTION WAVEFORM PREDICTION PROCEDURE	5. TYPE OF REPORT & PERIOD COVERED: Final Report for Period 25 Jun 79—15 Mar 80
	6. PERFORMING ORG. REPORT NUMBER:
7. AUTHOR(s): G. M. Teraoka; N. Lipner	8. CONTRACT OR GRANT NUMBER(s): DNA 001-79-C-0401
9. PERFORMING ORGANIZATION NAME AND ADDRESS: TRW Defense and Space Systems Group, One Space Park, Redondo Beach, California 90278	10. PROGRAM ELEMENT, PROJECT, TASK AREA & WORK UNIT NUMBERS: Subtask H53BAXSX377-20
11. CONTROLLING OFFICE NAME AND ADDRESS: Director, Defense Nuclear Agency, Washington, D.C. 20305	12. REPORT DATE: 15 March 1980
	13. NUMBER OF PAGES: 58
14. MONITORING AGENCY NAME & ADDRESS(if different from Controlling Office)	15. SECURITY CLASS. (of this report): UNCLASSIFIED
	15a. DECLASSIFICATION DOWNGRADING SCHEDULE

16. DISTRIBUTION STATEMENT (of this Report)

Approved for public release, distribution unlimited.

17. DISTRIBUTION STATEMENT (of the abstract entered in Block 20, if different from Report)

18. SUPPLEMENTARY NOTES

This work sponsored by the Defense Nuclear Agency under RDT&E RMSS Code B344079462 H53BAXSX37720 H2590D.

19. KEY WORDS (Continue on reverse side if necessary and identify by block number)

Ground Motion
High Explosive Environment
Nuclear Environment

20. ABSTRACT (Continue on reverse side if necessary and identify by block number)

The single burst ground roll environment is important to the prediction of the multiple burst environment for MX. Recent studies carried out under the planning and review of the DNA-sponsored Data Analysis Working Group (DAWG) have led to an improved understanding of the phenomenology of the upstream-induced environment component for both the outrunning and superseismic regions. While the process of developing prediction techniques is still evolving, the purpose of this study is to perform an evaluation of the current methodology. This report summarizes preliminary results of this evaluation.

DD FORM 1 JAN 73 1473 EDITION OF 1 NOV 65 IS OBSOLETE

UNCLASSIFIED

SECURITY CLASSIFICATION OF THIS PAGE (When Data Entered)

TABLE OF CONTENTS

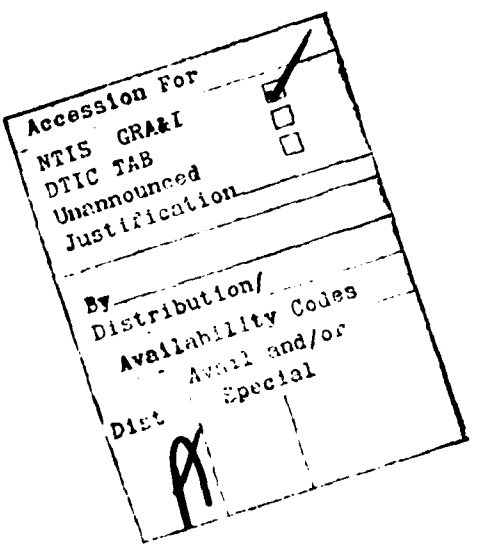

LIST OF ILLUSTRATIONS

LIST OF ILLUSTRATIONS (continued)

1.0 INTRODUCTION

The surface burst ground motion environment is considered to consist of components associated with the local airslap loading and with the upstream loading, including the upstream airblast and direct coupling of energy near ground zero, as is shown in Figure 1. Close-in, the direct coupling of energy has a significant effect on the upstream-induced component and results in a large displacement low frequency response. At long range (i.e., low overpressure) from a nuclear detonation, the upstream-induced environment is a low frequency oscillatory surface wave, termed ground roll. The airslap-induced component is generally a higher frequency response.

Nuclear data in the outrunning region, including characteristic waveforms, were summarized by Sauer [1964]. This work formed the basis for outrunning motion predictions in the Air Force Design Manual [Crawford, et al., 1974]. During the Army Site Defense Programs, which considered low overpressure design environments, the ground roll environment was studied extensively by the Waterways Experiment Station (WES) [Joachim 1973; Hadala 1973]. These efforts concentrated primarily on the surface tangent high explosive events performed at the Defense Research Establishment, Suffield (DRES) and were the basis for development of a WES computer program for prediction of ground motion environments. Analyses of the ground roll environment for several subsequent high explosive events were performed by Higgins and Schreyer [1975]. Additional studies of the nuclear data were performed by Cooper [1972] and by Lipner, et al. [1975].

The single burst ground roll environment is important to the prediction of the multiple burst environment for MX. Recent studies carried out under the planning and review of the DNA-sponsored Data Analysis Working Group (DAWG) have led to an improved understanding of the phenomenology of the upstream-induced environment component for both the outrunning and superseismic regions. While the process of developing prediction techniques is still evolving, the purpose of this study is to perform an evaluation of the current methodology. This report summarizes preliminary results of this evaluation.

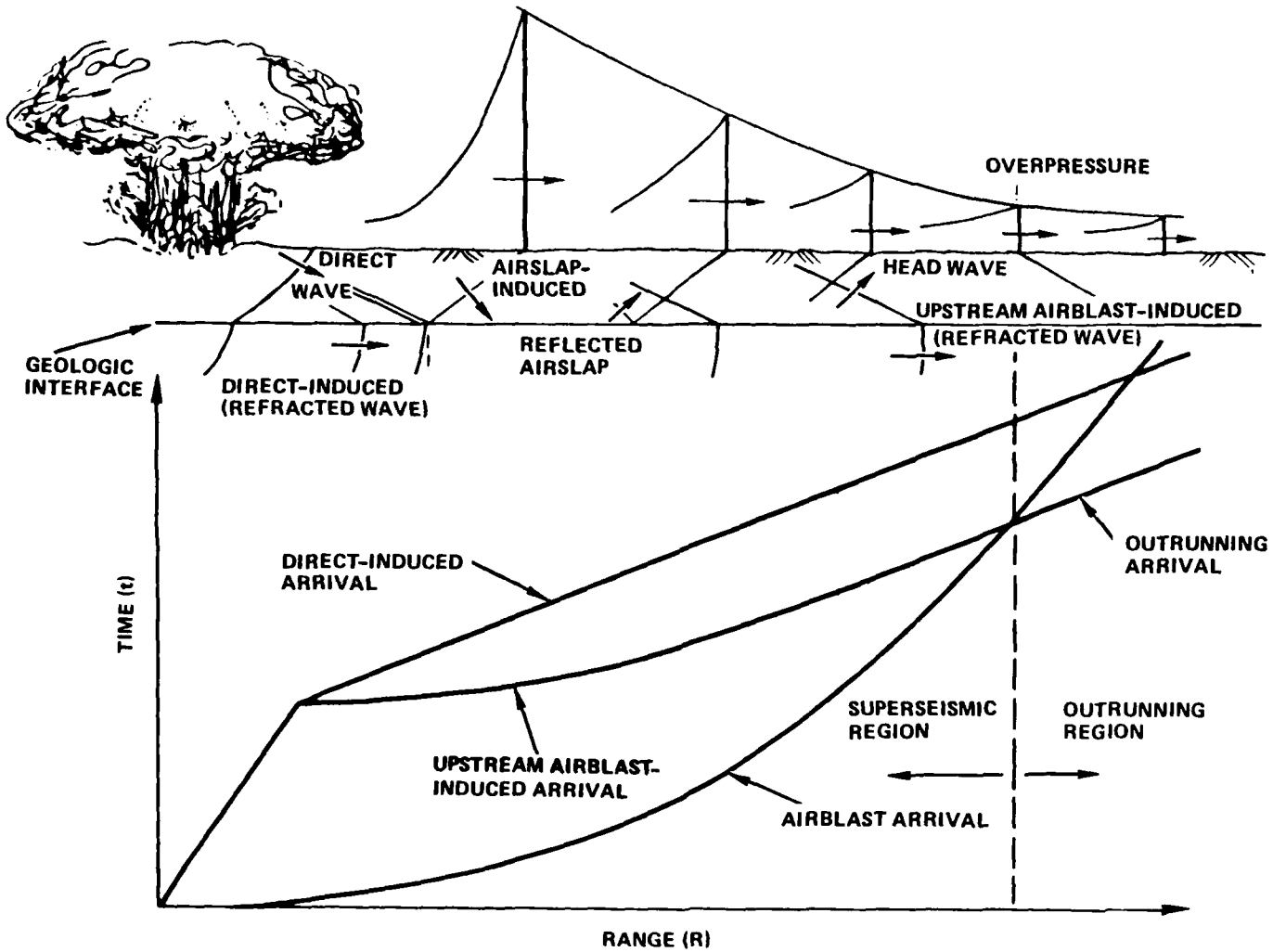

Figure 1. Surface Burst Ground Shock Phenomenology for Layered Geology

2.0 GROUND MOTION DEFINITIONS

An approach to analysis of ground motions is to separate the response into individual components. Even though there are nonlinear interactions between components which do not allow for such separation on a mathematically precise basis, it is a useful engineering approach because the resulting errors are well within the overall uncertainties of the problem and it is then possible to account for each part of the motion.

2.1 GROUND SHOCK COMPONENTS

When the airblast is superseismic, i.e., the shock-front velocity is traveling faster than the compressive stress wave speed in the layer, the initial ground shock response will be caused by the airblast in the immediate vicinity of the point of interest. This ground shock component is termed airslap-induced (Figure 1).

At the interface between the two geologic layers, some of the energy of the incident airslap-induced wave is reflected back into the upper layer and some is transmitted into the lower layer. As the airblast shock-front velocity slows, a refracted wave in the lower stiffer layer begins to outrun the airslap-induced ground shock and drive a head wave into the upper layer. Surface outrunning occurs beyond the range where the head wave arrives at the surface before the airblast.

Ground shock associated with all sources other than the local airblast (including directly coupled energy and upstream airblast) is termed upstream-induced ground shock [V4 Working Group, 1980]. Thus, this definition includes both effects generated by the energy coupled at the burst point and effects from upstream airblast loading.

2.2 UPSTREAM-INDUCED WAVEFORM PREDICTION

The prediction equations for this waveform component, as recommended by the DAWG [1978], are provided in Appendix A. The waveform is a series of exponentially decaying trigonometric functions, as shown in Figure 2. Two parameters are required to completely define the vertical and horizontal ground motion histories: the peak velocity (vertical and horizontal values are taken to be equal) and the period of horizontal motion. In the close-in

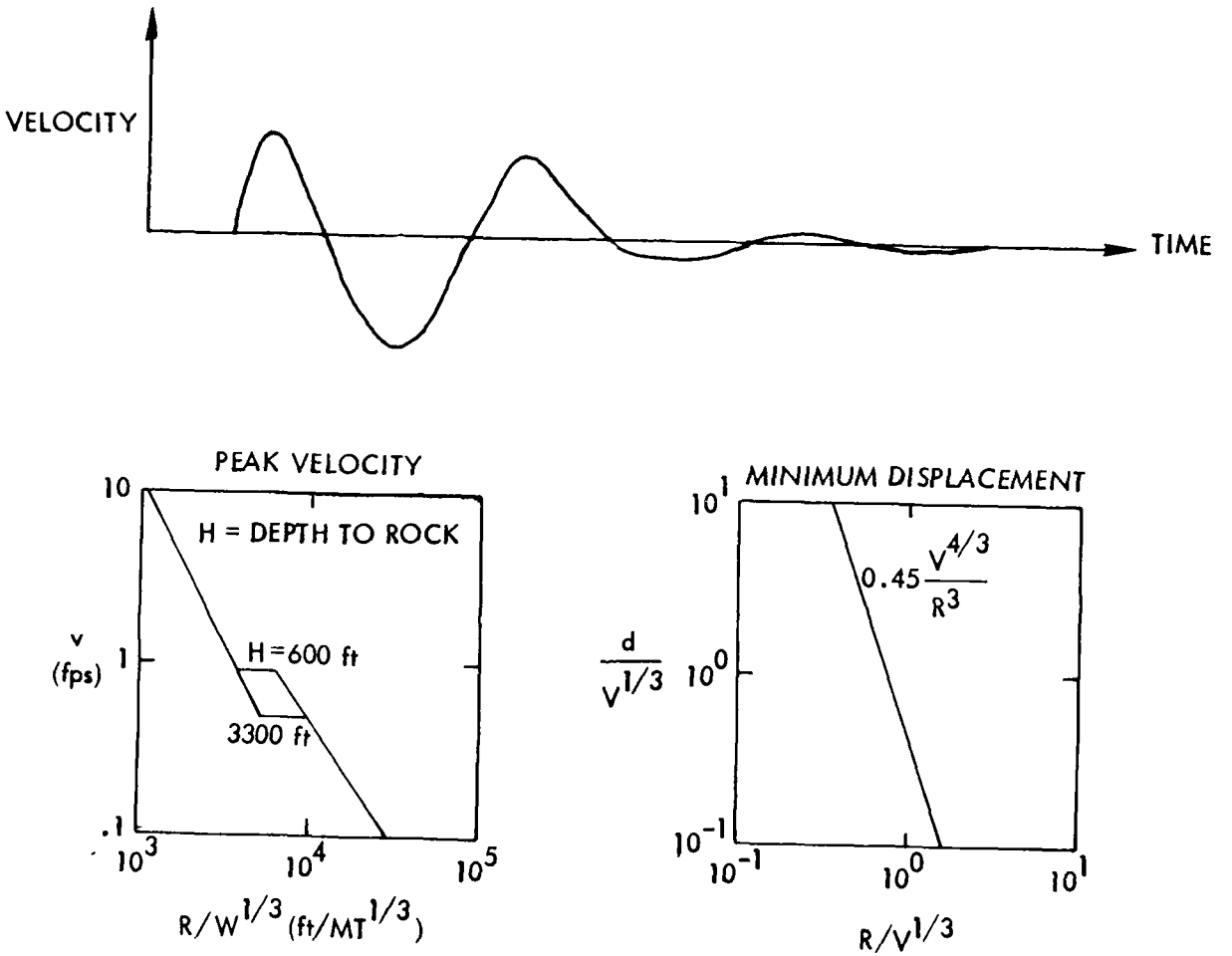

Figure 2. DAWG Upstream-Induced Waveform Definition

region, the period is adjusted consistent with the large displacements associated with direct-induced effects.

The prediction of peak velocity is site independent, except within a region which is near or contains the outrunning range. This region has a constant peak velocity (thus is termed the plateau region) dependent on the depth to rock (H). The peak velocity prediction here is given by 0.75 fps $[1000 \text{ ft/H}]^{1/3}$.

The primary response period [Murphy, Bennett 1980] is $2H/C_{S1}$ (C_{S1} is the depth-weighted-average shear wave speed of the soil above the rock), except when this results in a horizontal displacement less than the Cooper crater volume scaling prediction of $0.45V^{4/3}/R^3$ (V is the apparent crater volume and R is the range from the weapon). The horizontal displacement is then forced to be equal to this value by increasing the period. Vertical and horizontal displacements are slightly different close-in, however, at long range both have identical waveforms.

The basis for development of this waveform is as follows:

DAWG Waveform Parameter	Basis
Peak velocity at close-in ranges	WES analysis of high explosive data [DAWG 1978]
Peak velocity in plateau region	Finite element computer code calculations for various depths to rock [Sandler 1978]
Peak velocity at long range	Analysis of nuclear data [Lipner, et al., 1975]
Surface wave period	Elastic surface wave analysis [Auld and Murphy 1979]
Arrival time	Seismic calculation using shear wave speeds of the media

3.0 DAWG UPSTREAM-INDUCED WAVEFORM EVALUATION

The development of the DAWG waveform involved an extension of work performed by WES for the Army Site Defense studies. While the WES work was based largely on data from the DRES high explosive events (e.g. PRAIRIE FLAT and DIAL PACK), the more recent analyses within the DAWG have focused more on Event 6 from the PRE-MINE THROW IV series and on PRE-DICE THROW II, Events 1 and 2. To provide an evaluation of the waveform for a different geology, the 100 ton MIDDLE GUST III and IV events were considered in this study.

Since computer code calculations have been gaining increased credibility in predicting ground motions, through studies of the PRE-MINE THROW IV and PRE-DICE THROW II events, comparisons with finite difference nuclear calculations were also performed in this evaluation of the DAWG waveform. These calculations [Sandler 1978] considered a 1 MT surface burst airblast loading on two MX-related geologies, with depths to rock of 600 and 1000 ft.

3.1 PEAK VELOCITY PREDICTIONS

The high explosive data base that WES used to develop the peak velocity prediction, for the DAWG waveform, at close-in ranges is shown in Figures 3 and 4 along with the nuclear prediction curves. In their studies, WES used an equivalent yield factor of one-half in analysis of high explosive data for purposes of nuclear predictions. The horizontal velocity data do not have very large variations over a large range of geologies and the prediction curve is slightly above the median of the data. The vertical velocity data exhibit scatter that ranges - from top to bottom - from factors of about 3.5 to 7, with the prediction nearer the median of the data. The PRE-MINE THROW event was conducted in a relatively homogeneous geology with a large depth to water table and rock. Close-in vertical velocity data for this event are near the bottom of the scatter. Data for the DRES events, conducted in a geology with about a 23-ft depth to water table, generally tend to be above the close-in prediction line. This difference may be associated with the fact that the layering in the Suffield events result in upstream-induced head waves which propagate upward from the water table into the overlying dry soil. Because of the impedance mismatch between the wet and dry soil materials, the compression head waves have a fairly shallow wave front angle. Thus, if the primary response is in this wave the vertical velocity would be

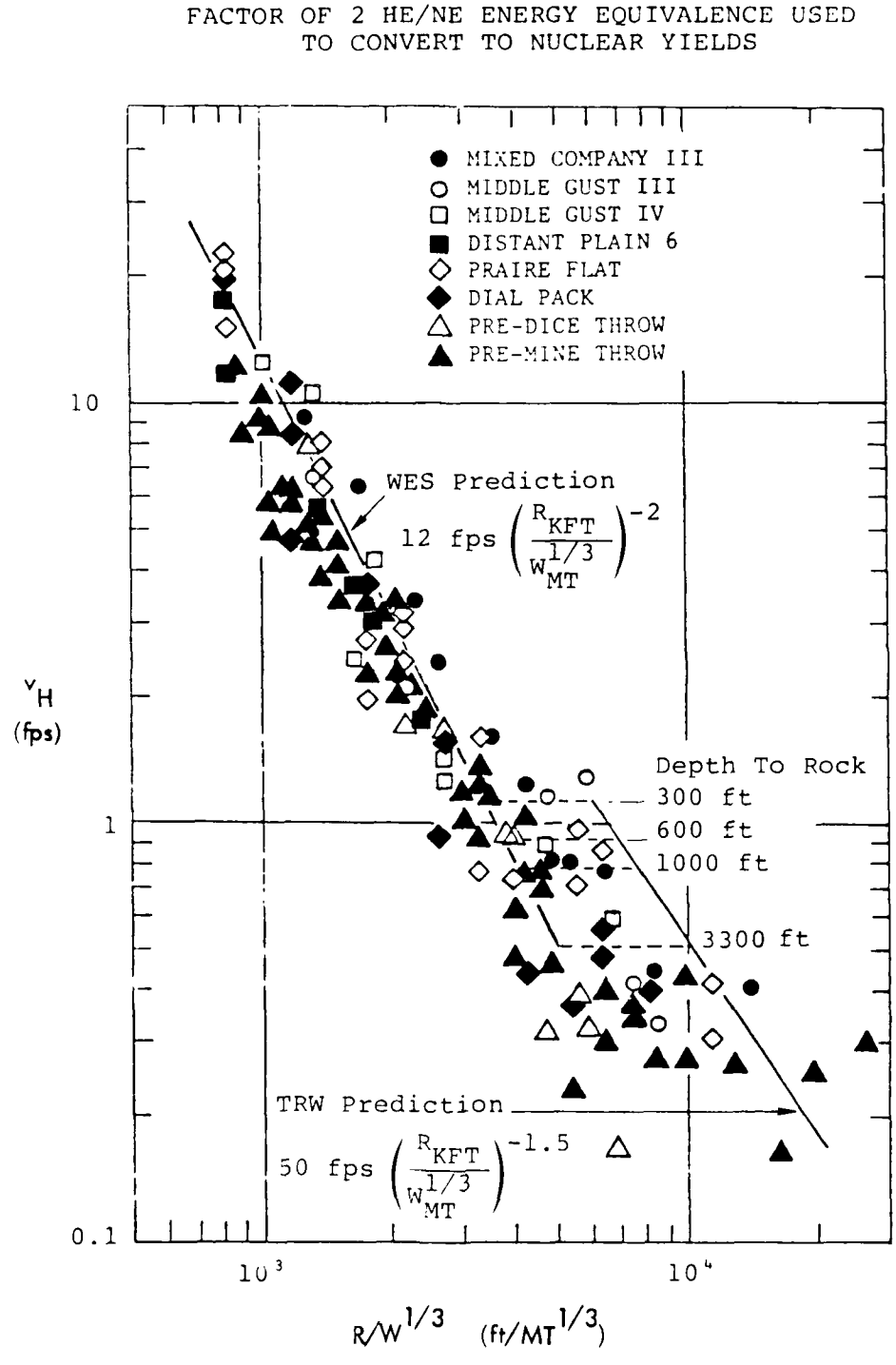

Figure 3. Peak Upstream-Induced Horizontal Velocity [DAWG]

FACTOR OF 2 HE/NE ENERGY EQUIVALENCE USED
TO CONVERT TO NUCLEAR YIELDS

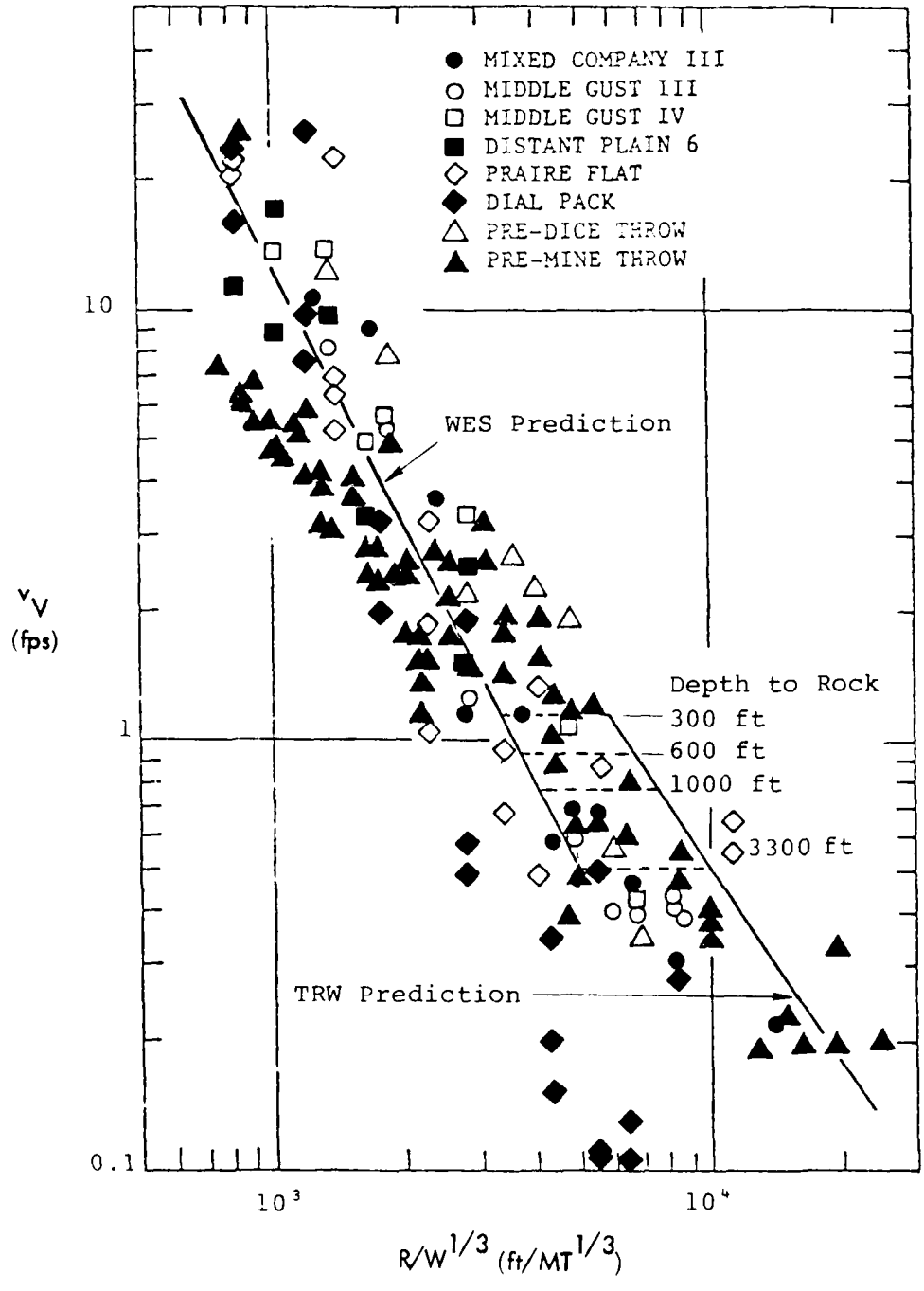

Figure 4. Peak Upstream-Induced Vertical Velocity [DAWG]

larger than the horizontal. Because of the more uniform PRE-MINE THROW geology, significant head waves would not develop.

To use a basis for quantification of uncertainties in the high explosive data and to study test events individually, a regression analysis of peak horizontal velocity data was performed. This analysis included all strong motion data, for several events, in the vicinity of the 1.5 ft depth. Calculations were first performed for all gage ranges and then for only those ranges within the outrunning radius, R_o. A direct evaluation of the close-in prediction could be made from the superseismic results. An additional source of uncertainty is in the equivalent yield factor, which was not evaluated in this study.

The regression analysis was a least square fit to the equation

$$v_H = A \left[\frac{R}{W^{1/3}} \right]^{-n} \qquad (1)$$

with the results shown in Table 1. In addition, those data in the 2.5% extremes on both sides of the distribution were dropped and the regression analysis repeated (these results are given in the second row corresponding to a test event). However, the only value of this information is to show the impact of data at the extremes - any data that are actually dropped should be excluded only as a result of evidence which shows that they are not correct. Also shown in the table are (a) regression analysis velocity prediction (v_1) for a scaled range corresponding to approximately 600 psi overpressure, and (b) 90% K-Factors (factors which multiply and divide the median prediction to encompass 90% of the data; 5% left off on each end).

Except for MIXED COMPANY 3, the regression analysis results for each event were in good agreement with the DAWG prediction. However, there were some systematic differences between the events with shallow rock (MIDDLE GUST III and IV and MIXED COMPANY 3) and with deep rock (PRAIRIE FLAT, DIAL PACK, DISTANT PLAIN 6, AND PRE-DICE THROW II-1 and 2). The shallow rock predictions for v_1 vary from 4.4 to 6.4 fps (average value of 5.1 fps), while the deep rock corresponding values vary from 3.8 to 4.3 fps (average of 3.7 fps). Thus, the horizontal velocities for the shallow rock geologies are higher by an average factor of about 1.4. A comparison between the DAWG

Table 1. High Explosive Peak Horizontal Velocity Regression Analysis

TEST	YIELD tons	R_o ft	ALL RANGES				SUPERSEISMIC			
			A fps	n	v_1 fps	90%K	A fps	n	v_1 fps	90%K
PRAIRIE FLAT	500	550	880	1.65	5.10	2.04	3330	2.13	4.31	1.49
			*1170	1.74	5.12	1.64				
DIAL PACK	500	550	800	1.74	3.50	1.73	1490	1.95	3.38	1.82
DISTANT PLAIN 6	100	420	930	1.88	2.63	1.88	1670	1.94	3.92	1.84
MIDDLE GUST III	100	230	490	1.49	5.64	2.99	1150	1.78	4.44	2.60
			530	1.49	5.06	2.00	550	1.50	5.09	1.98
MIDDLE GUST IV	100	300	790	1.65	4.58	1.91	1820	1.92	4.54	1.90
			770	1.65	4.46	1.83	1970	1.95	4.48	1.75
MIXED CO 3	500	300	1900	1.82	6.47	1.81	380	1.31	6.37	1.61
			1660	1.79	6.22	1.58	730	1.53	6.16	1.46
PRE-DICE TH II-1	100	280	530	1.61	3.48	2.10	5850	2.36	3.68	1.78
			570	1.63	3.51	1.92				
PRE-DICE TH II-2	100	280	490	1.65	2.83	2.14	5950	2.39	3.41	1.83
MINERAL ROCK	100		5280	2.26	4.55	1.82				
MINE ORE	100		7160	2.38	4.24	1.86				
			8550	2.43	4.33	1.63				

$$v_H = A\left[R_{ft}/W_{tons}^{1/3}\right]^{-n} \qquad v_1 = v_H\left[22.7\,ft/ton^{1/3}\right]; \sim 600\ psi$$

90% K Factors – Factors which multiply and divide the median prediction to encompass 90% of the data.

*When second row is listed, those data in the 2.5% extremes on both sides of the distribution were dropped and the regression analysis repeated.

horizontal velocity predictions and the data used in this analysis is provided in Figure 5, with results for the shallow rock geologies shown separately from those for the soil geologies. Except for the MINERAL ROCK and MINE ORE events (shown for comparison), all data are from the superseismic region. An assumption of the analysis is that this region is approximately the same as the close-in region. Future studies should also consider regression analysis of the vertical velocity data.

The upstream-induced velocity prediction at long range was originally based on vertical velocity data from one nuclear event at the Nevada Test Site (TUMBLER 1) and one at the Pacific Proving Grounds (IVY MIKE). These data and nuclear predictions, including two different estimates of the transition velocity (v_p) for IVY MIKE, are shown in Figure 6. The upstream-induced velocity was taken as the peak value during the non-airslap portion of the response. The top value is the DAWG prediction, while the bottom is a modification which considers a yield scaled depth to rock, viz.,

$$v_p = 0.75 \text{ fps} \left[\frac{1000 \text{ ft}}{H} \quad W_{MT}^{1/3} \right]^{1/3} \qquad (2)$$

The need for a modification of this type follows from geometric scaling rules. This correction, which is not very sensitive to yield, is only a factor of 1.3 for the 10.4 MT IVY MIKE event.

Horizontal velocity data for several NTS nuclear events are also shown in Figure 6 along with both predictions for the NTS plateau velocity. (These predictions considered the Yucca Flat geology, but values for Frenchman Flat would only differ slightly.) The yield correction makes a difference of a factor of 2 for 1 kT, which typifies the yields of these NTS events. The horizontal velocity data are in reasonable agreement with prediction. There is actually better agreement for the uncorrected plateau velocity, but the data in the plateau region are from buried bursts (JANGLE U and JOHNIE BOY). Therefore, a definitive conclucion regarding the plateau velocity cannot be reached.

Some of the high explosive events had seismic measurements out to relatively long range, including PRAIRIE FLAT, MIDDLE GUST IV, PRE-DICE THROW II-1, and MISERS BLUFF II-1. These data provide additional evaluation of the low overpressure predictions. MIDDLE GUST IV data (using a factor of

FACTOR OF 2 HE/NE ENERGY EQUIVALENCE USED TO CONVERT TO NUCLEAR YIELDS

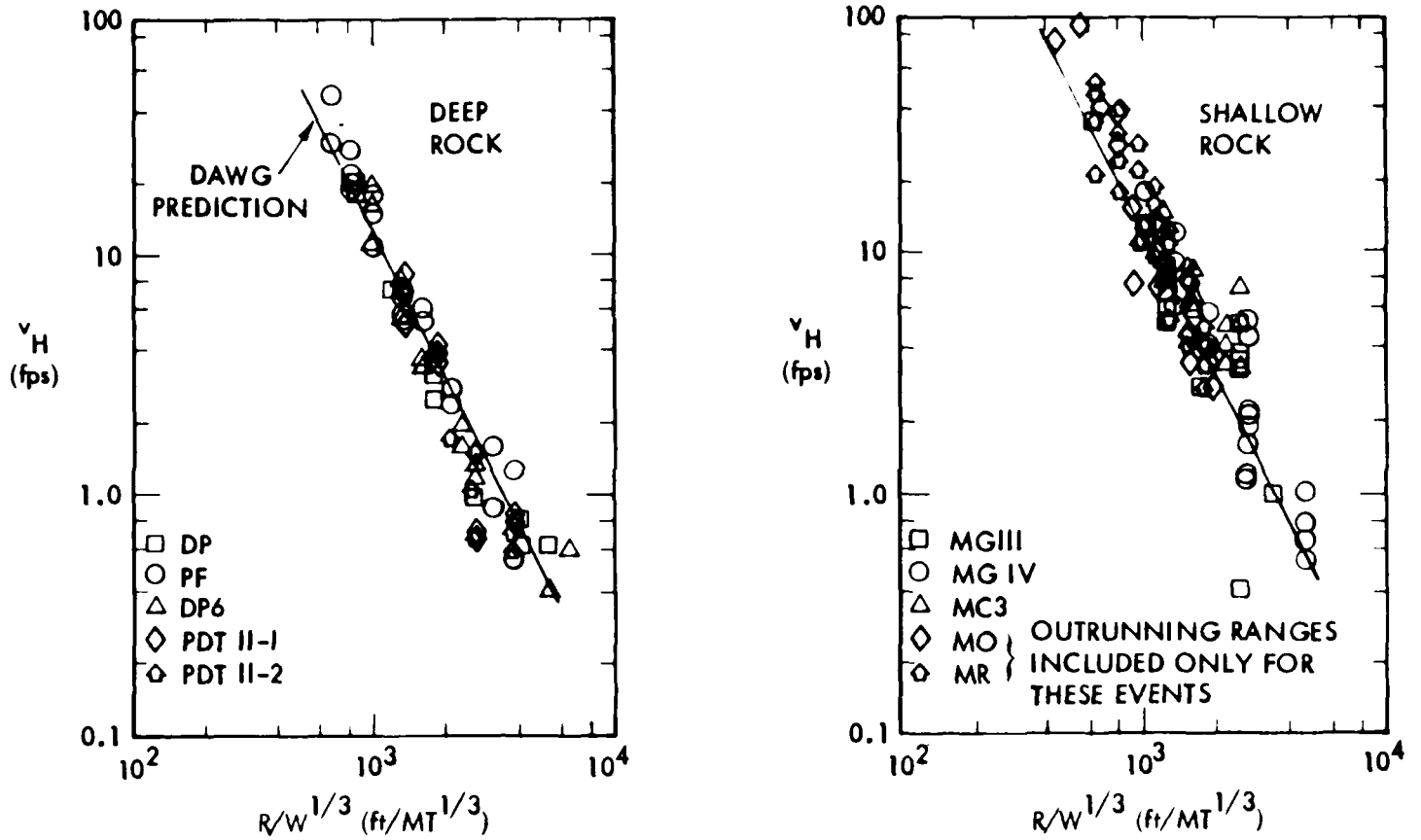

Figure 5. Peak Horizontal Velocity In Superseismic Region (~1.5 ft Depth)

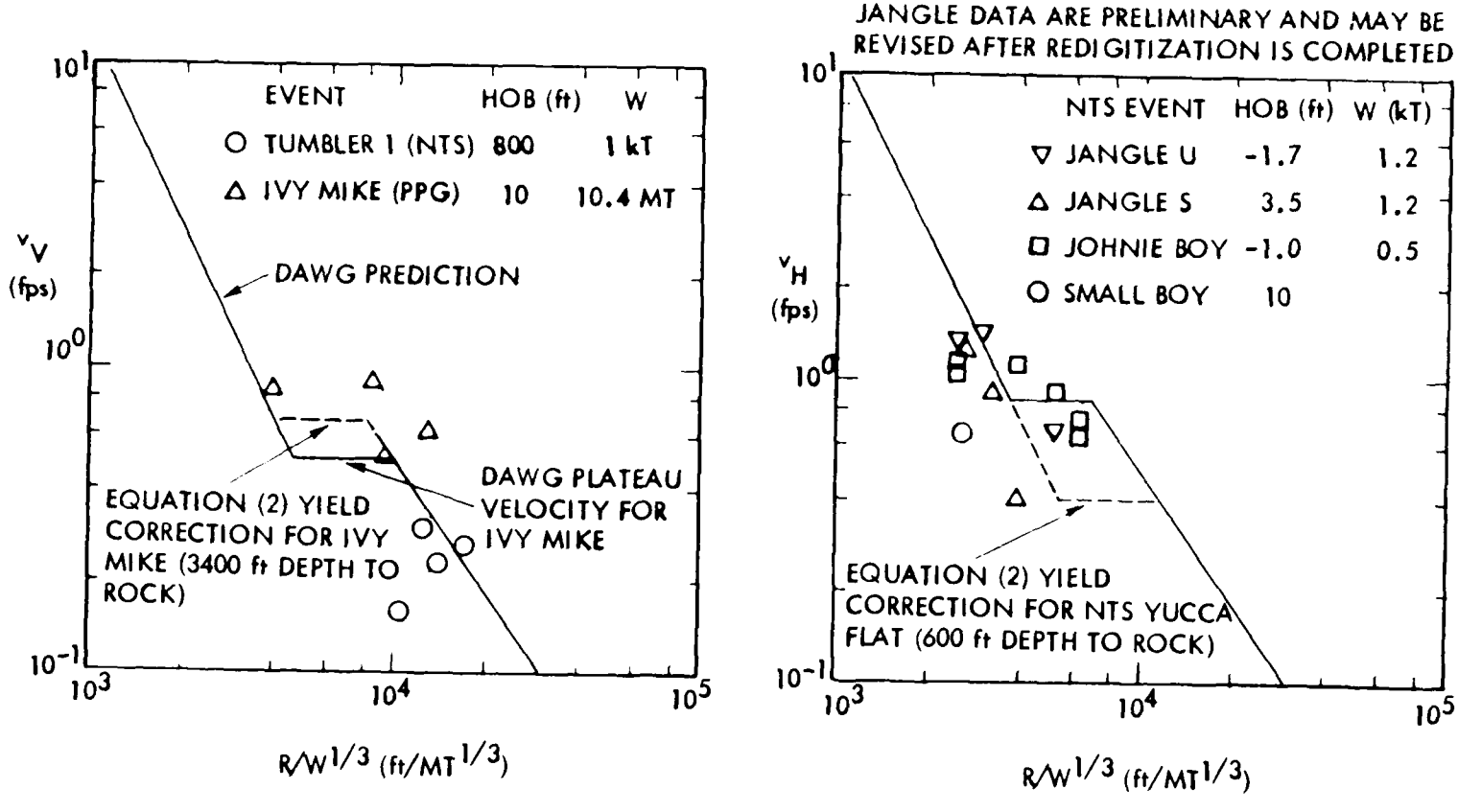

Figure 6. Peak Upstream-Induced Near-Surface Velocity

two HE/NE equivalence), shown in Figure 7, are substantially larger (factor of 5 or greater) than the prediction. In addition, there was a late-time dominant high frequency (order of 5 Hz) response at the seismic stations, which propagated outwards at about 1650 fps.

A similar type of response (but lower frequency, on the order of 1-2 Hz) was observed in the PRE-DICE THROW II event. In that case it was identified as a fundamental mode Rayleigh wave. However, this does not imply that MIDDLE GUST IV has a similar phenomenology. To further investigate the phenomenology of this response, elastic surface wave analyses of the MIDDLE GUST IV event should be performed. These types of calculations proved useful in the investigation of PRE-DICE THROW II-1 and PRE-MINE THROW IV-6 events. Finite difference calculations would also be of value, but the zoning required to capture the 5 Hz response would be costly.

3.2 WAVEFORM COMPARISON

Comparisons of the DAWG prediction waveform with finite difference calculations are presented in this section. A summary of the site properties used in the Weidlinger Associates (WA) calculations [Sandler 1978] and in waveform predictions using the DAWG methodology is presented in Figure 8. The WA velocity and displacement time history calculational results are shown in Figure 9 and 10, with DAWG predictions overlayed at select ranges; while larger scale displacement comparisons are presented in Figures 11 to 17.

The two-dimensional WA calculations simulated airblast loading only and therefore did not account for direct-induced effects. To be consistent with this, a zero crater volume was used for the DAWG predictions. In comparing the two results, it should be noted that the WA calculations contain the complete airblast-induced response, while the DAWG predictions contain only upstream airblast-induced effects. Therefore, the predicted displacement histories were given initial values equal to those obtained from the WA calculation at the time of arrival of the upstream-induced signal.

The arrival time of the DAWG waveform is significantly behind that of the upstream-induced arrival for the WA calculations, because the first upstream arrival is calculated from the S-Wave speeds. The prediction should be revised to reflect a signal corresponding to P-Wave arrivals. A

FACTOR OF 2 HE/NE ENERGY EQUIVALENCE USED TO CONVERT TO NUCLEAR YIELDS

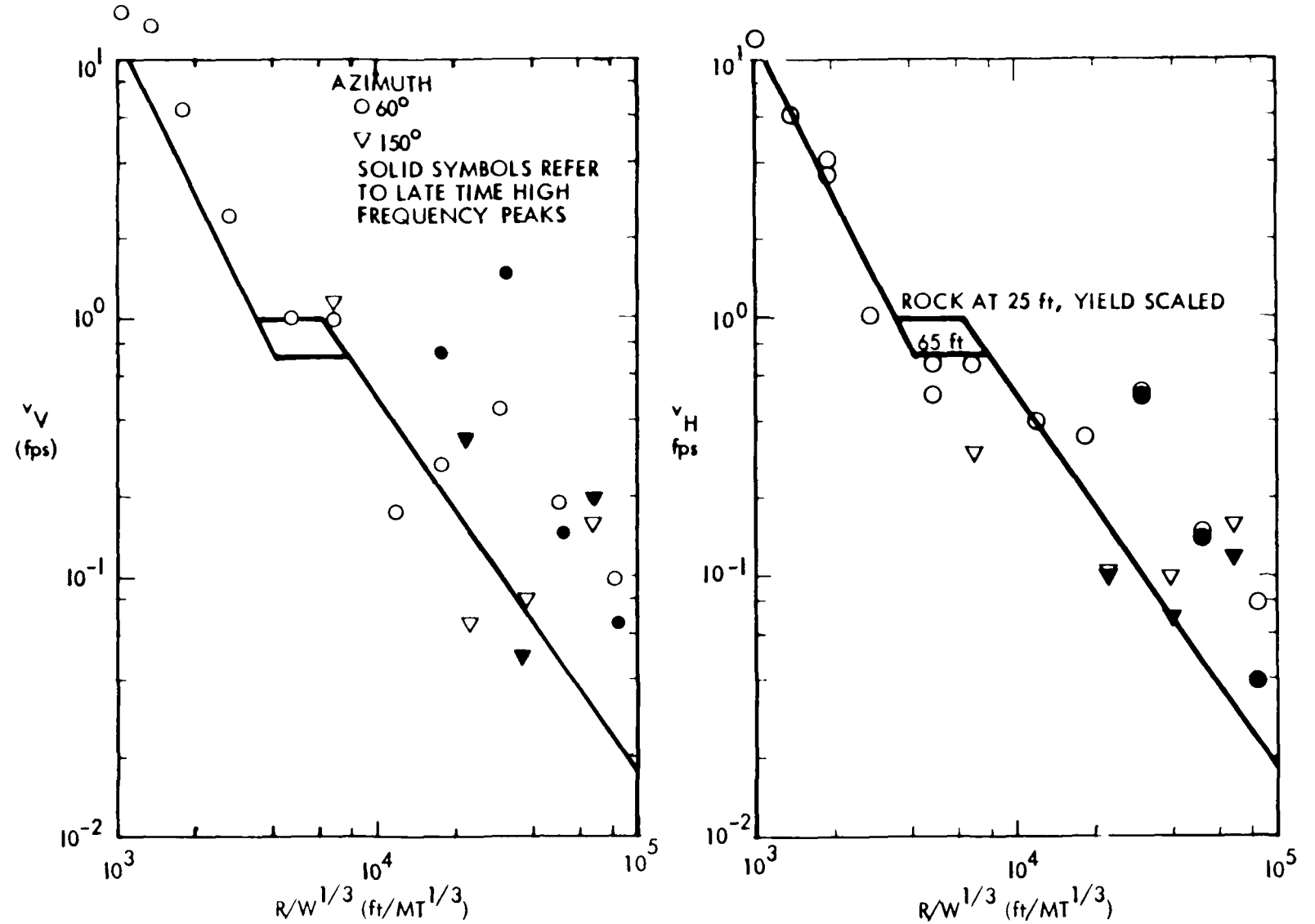

Figure 7. Middle Gust IV Upstream-Induced Peak Velocity

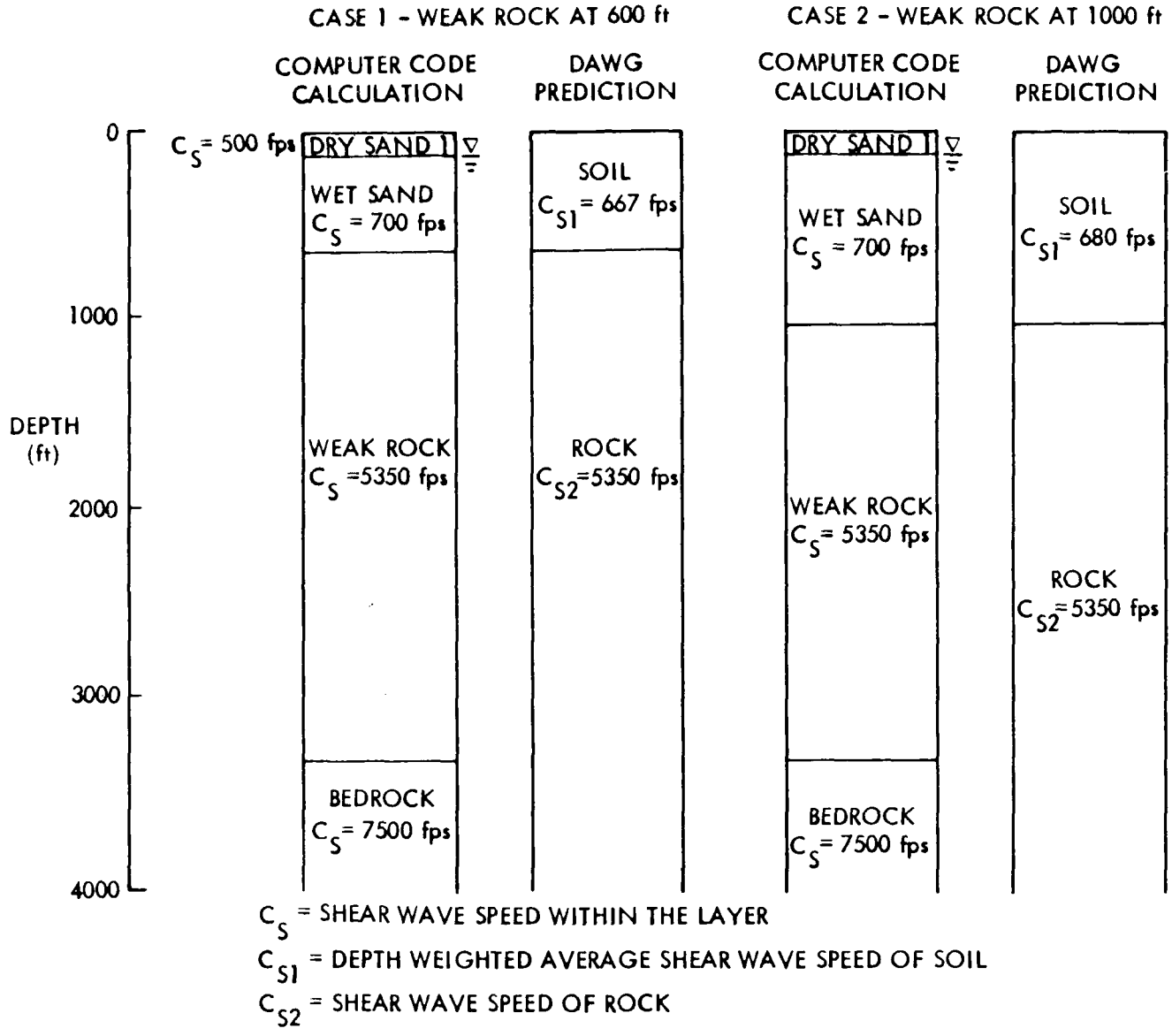

Figure 8. Site Properties for WA Calculations and DAWG Prediction Waveforms

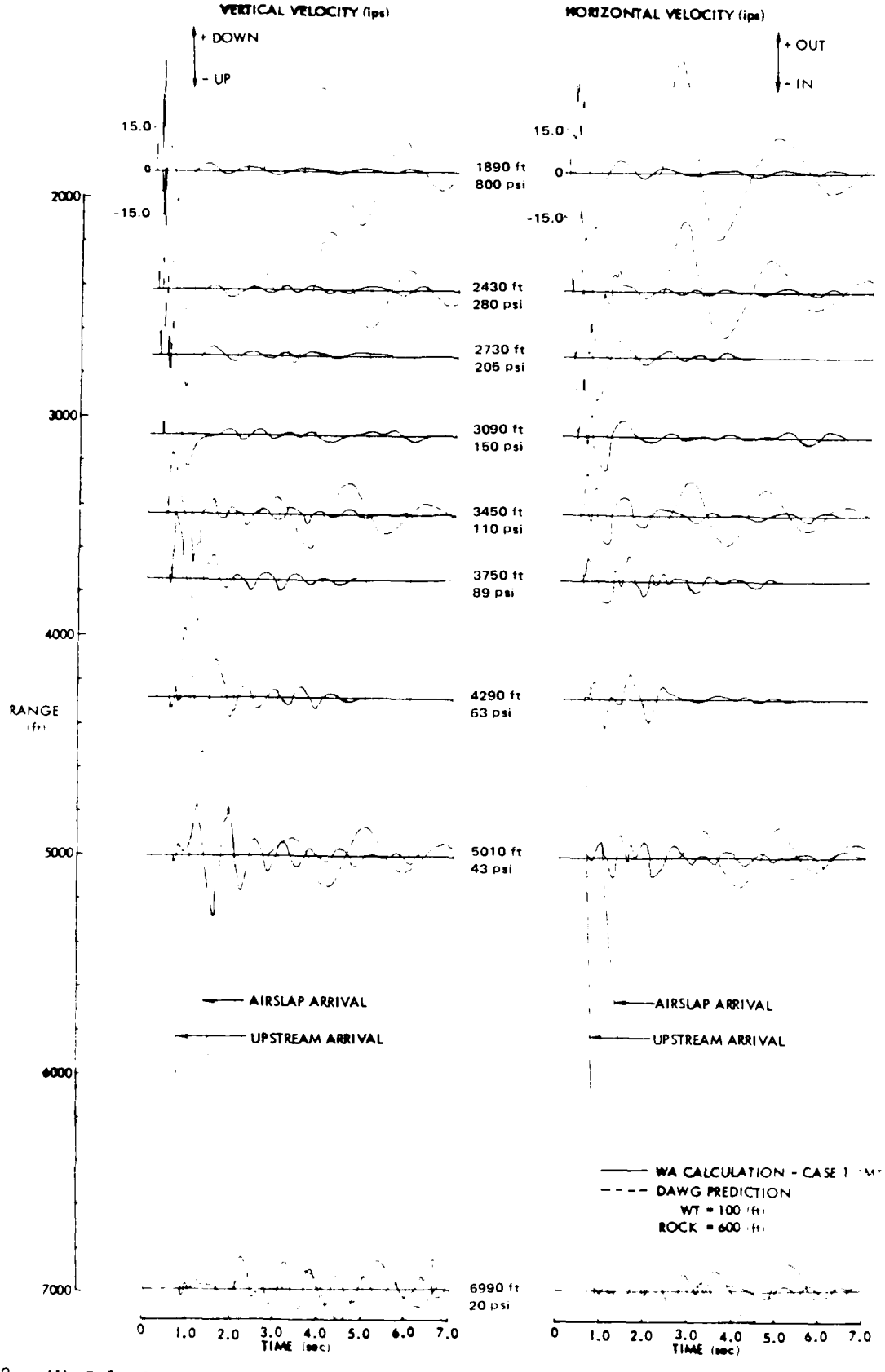

Figure 9. WA Calculation and DAWG Prediction Velocity Time History Comparison, Case 1

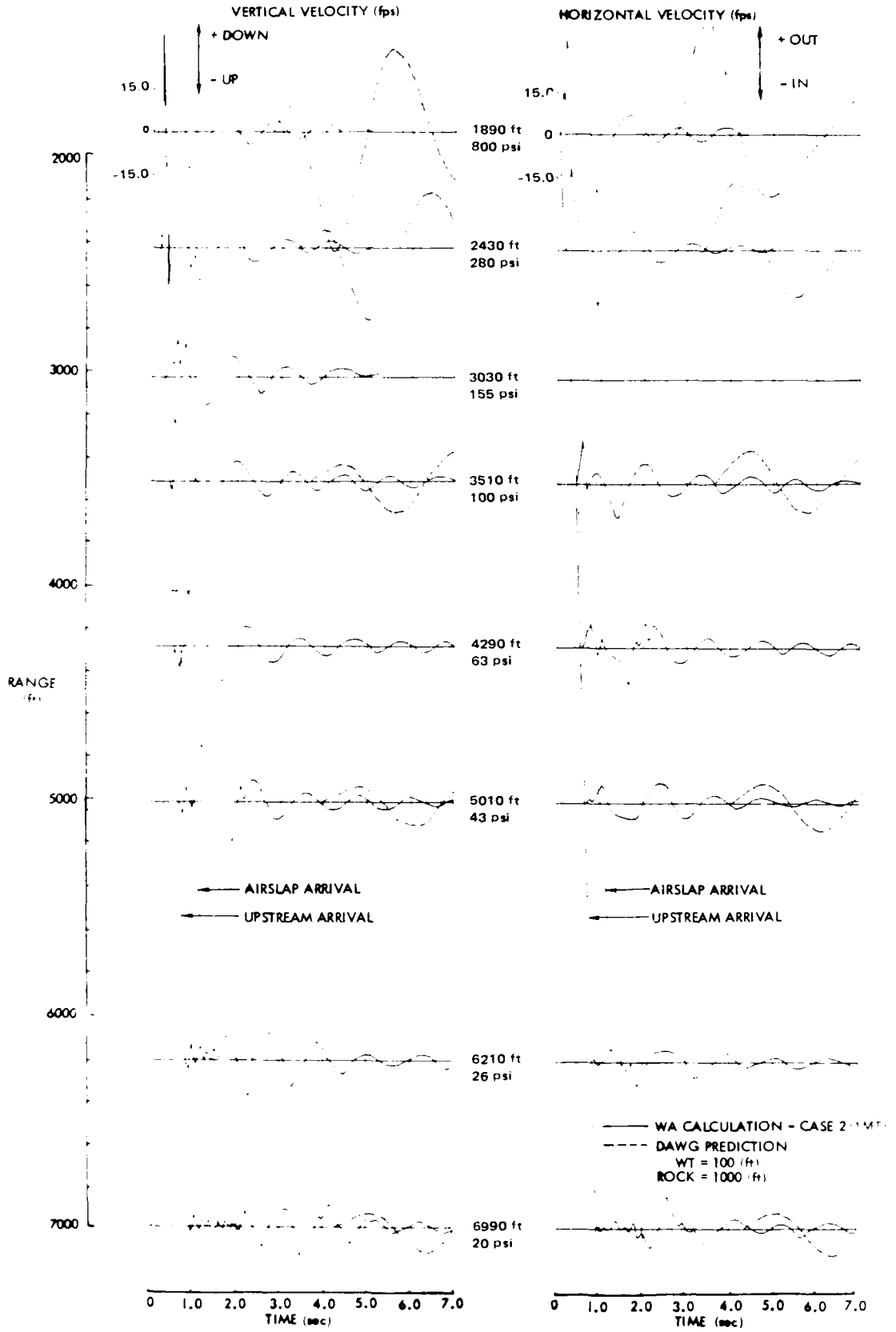

Figure 10. WA Calculation and DAWG Prediction Velocity Time History Comparison, Case 2

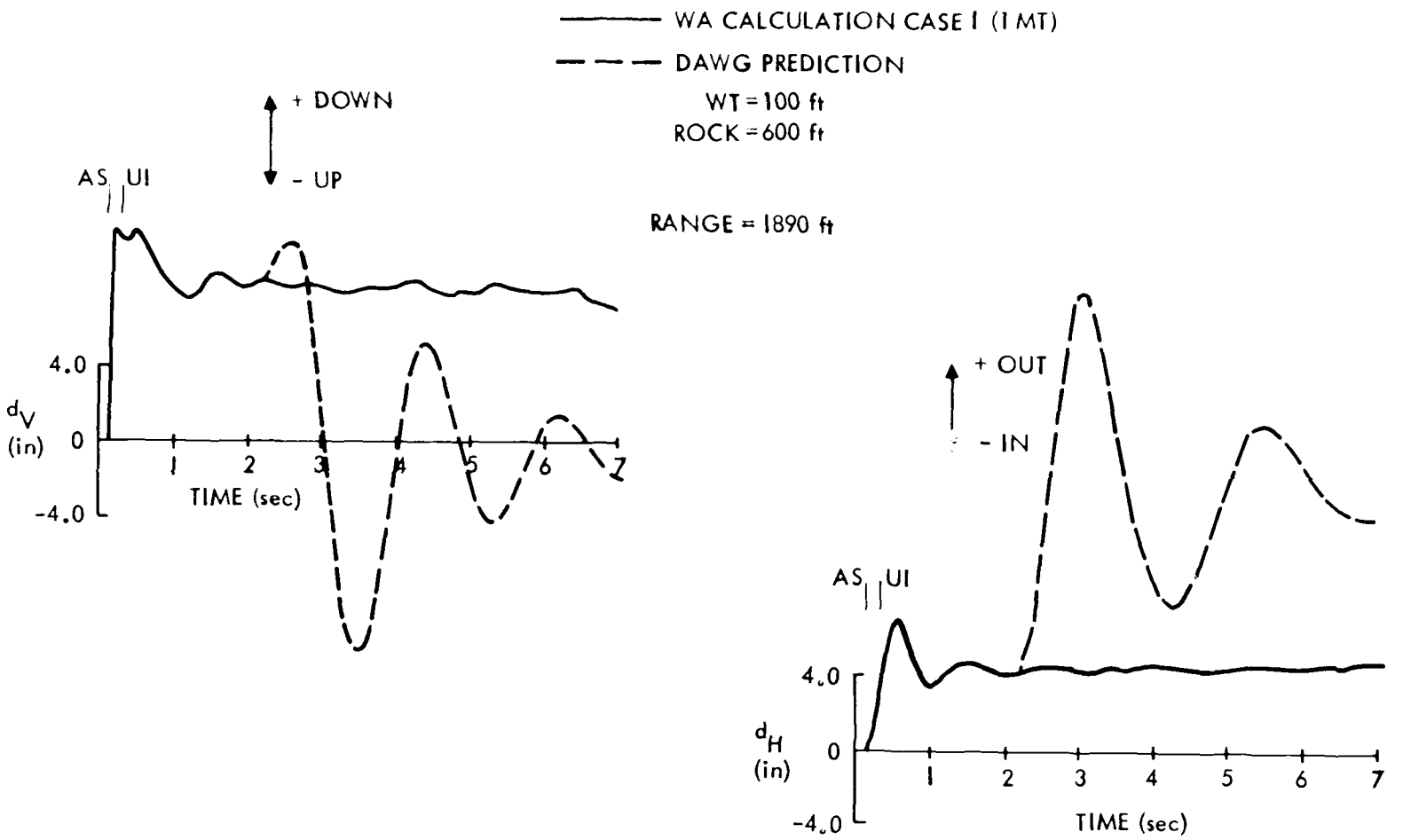

Figure 11. WA Calculation and DAWG Prediction Displacement Time History Comparison, Case 1, 1890 ft Range

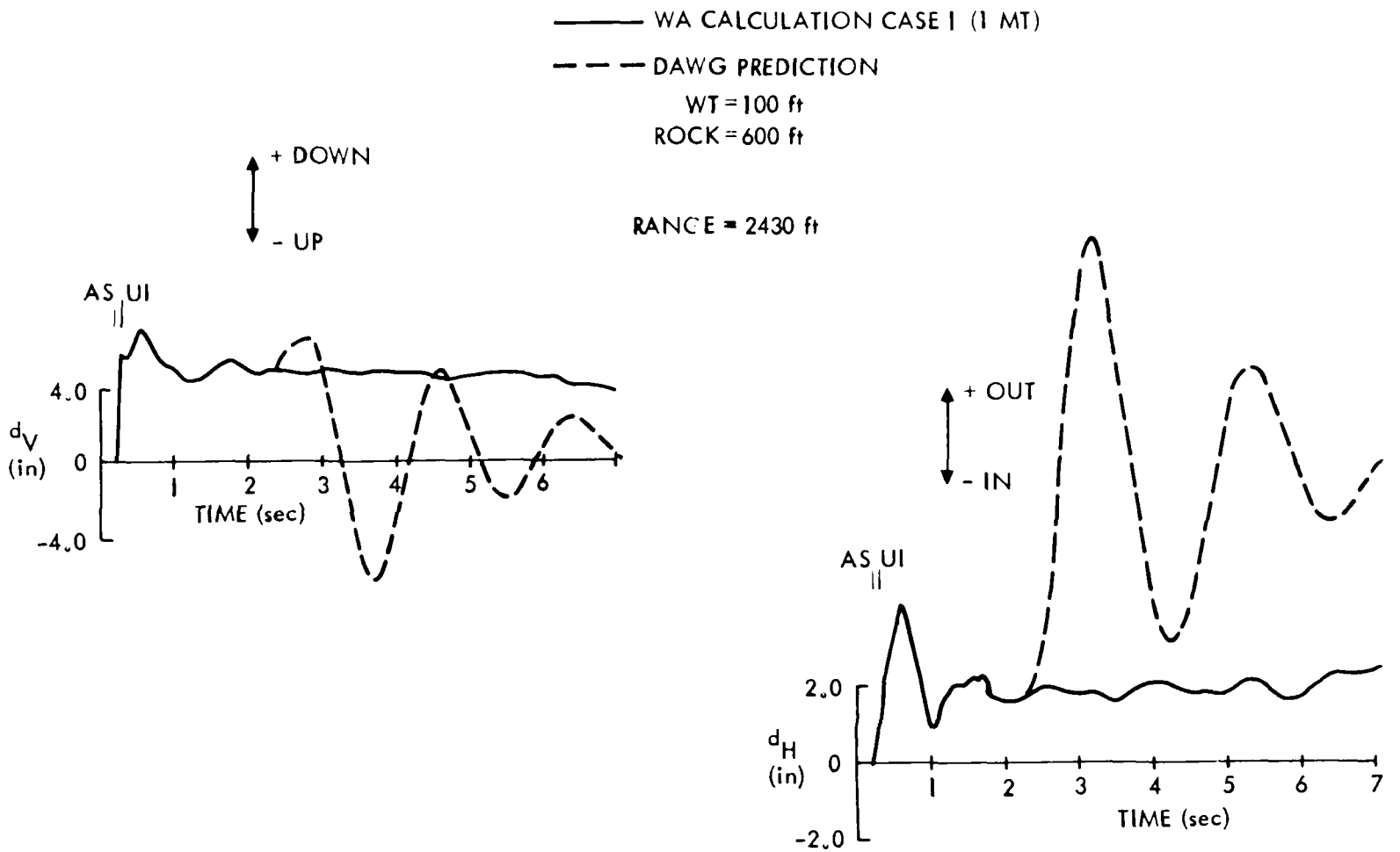

Figure 12. WA Calculation and DAWG Prediction Displacement Time History Comparison, Case 1, 2430 ft Range

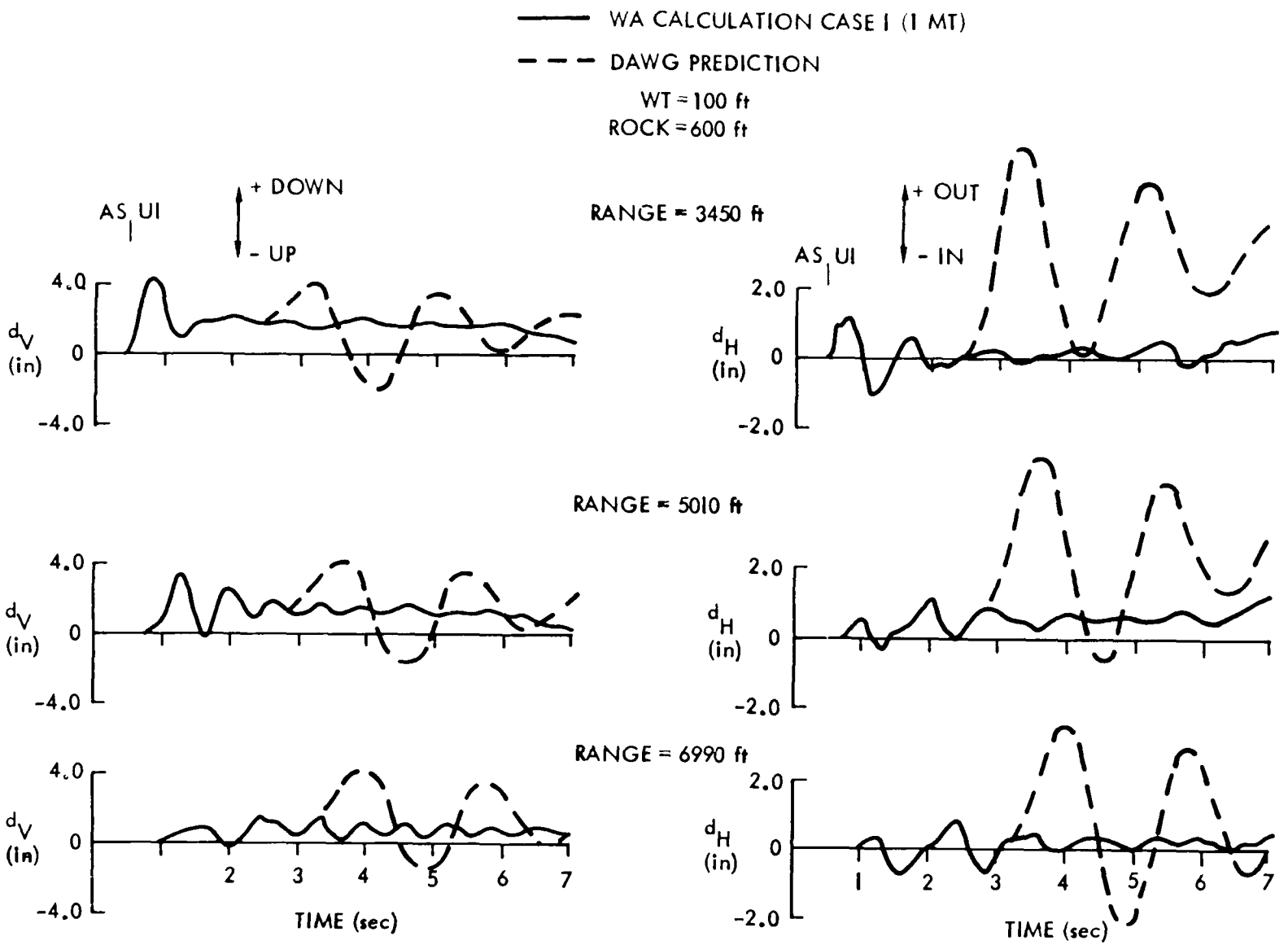

Figure 13. WA Calculation and DAWG Prediction Displacement Time History Comparison, Case 1, 3450, 5010 and 6990 ft Range

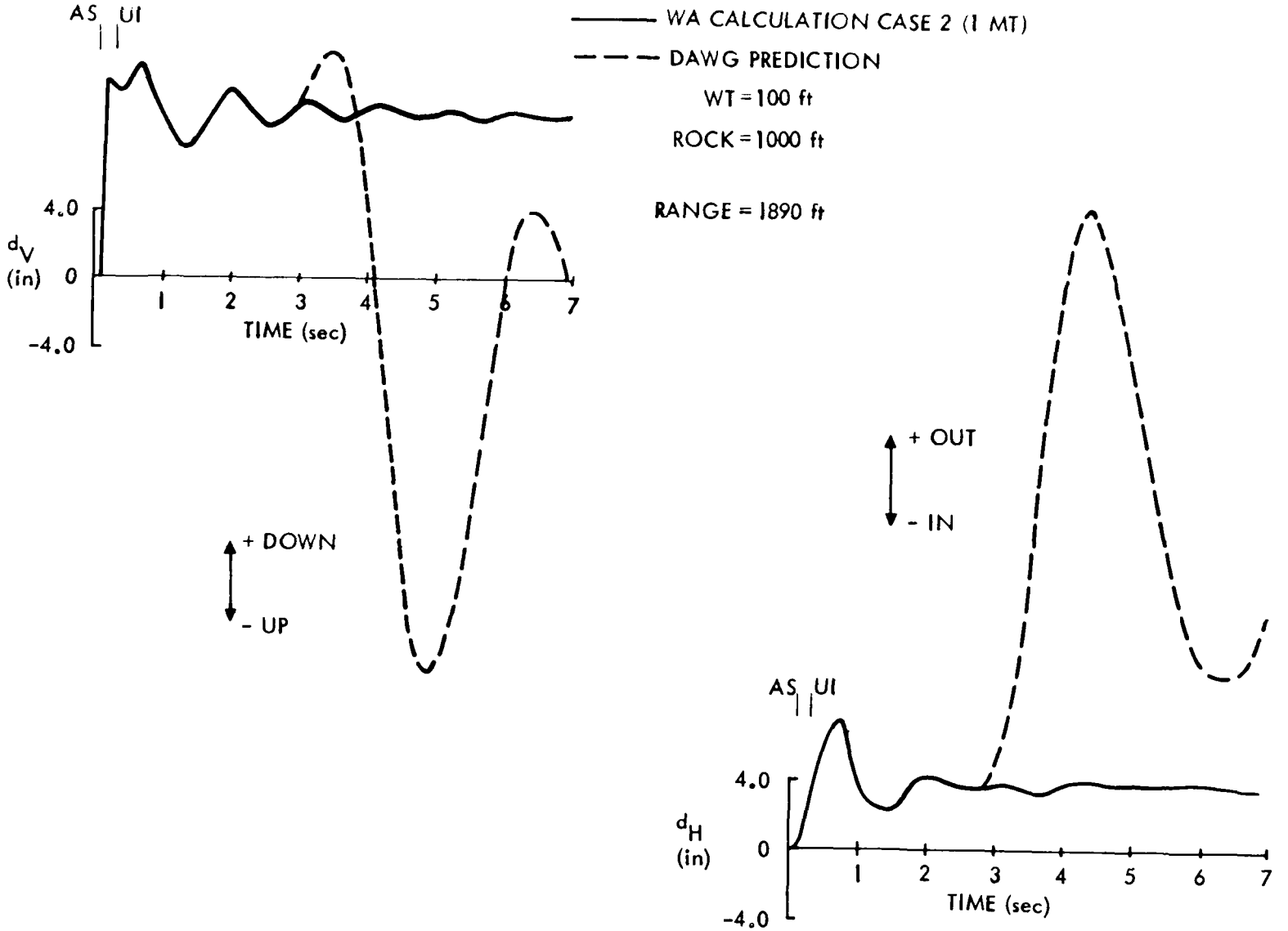

Figure 14. WA Calculation and DAWG Prediction Displacement Time History Comparison, Case 2, 1890 ft Range

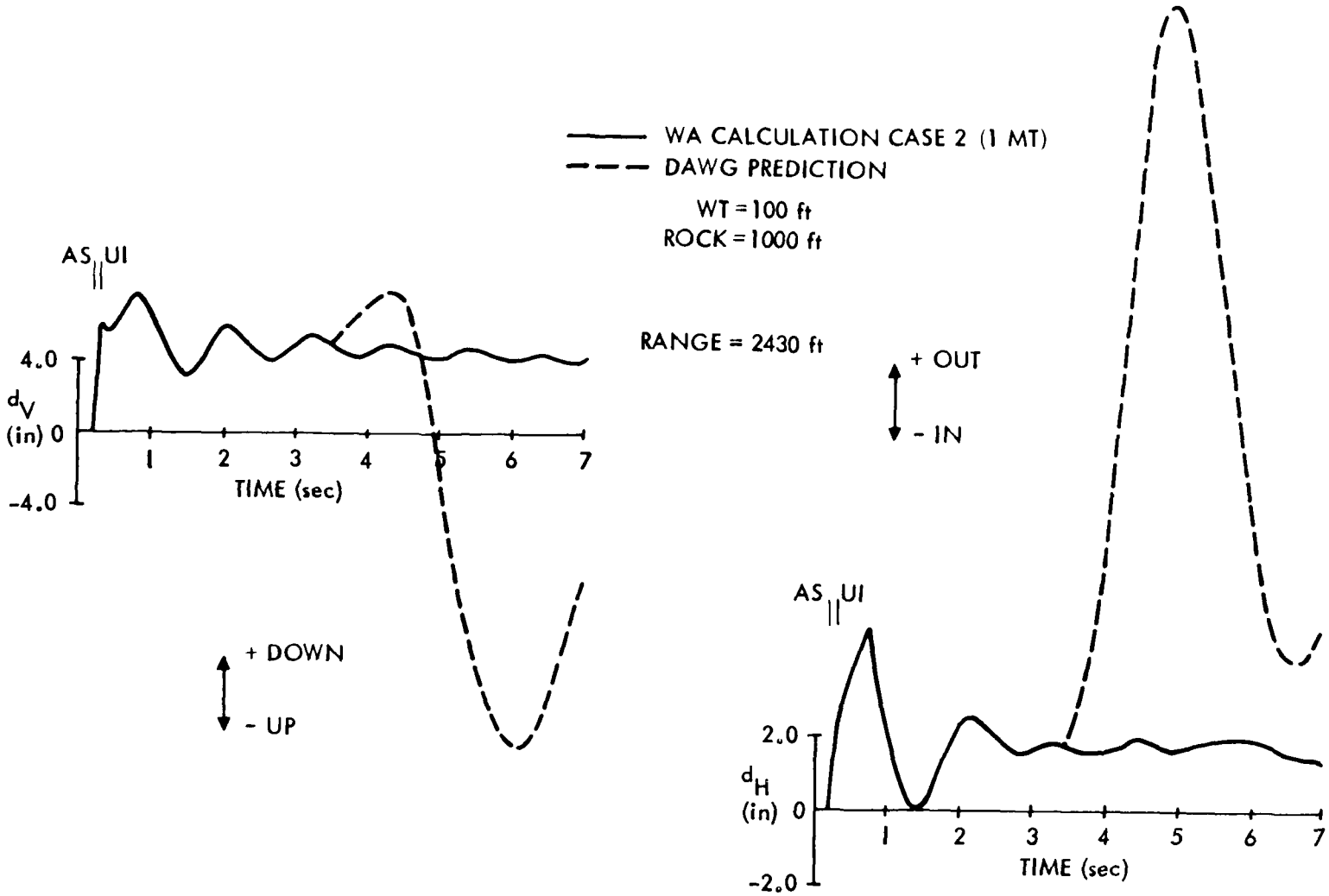

Figure 15. WA Calculation and DAWG Prediction Displacement Time History Comparison, Case 2, 2430 ft Range

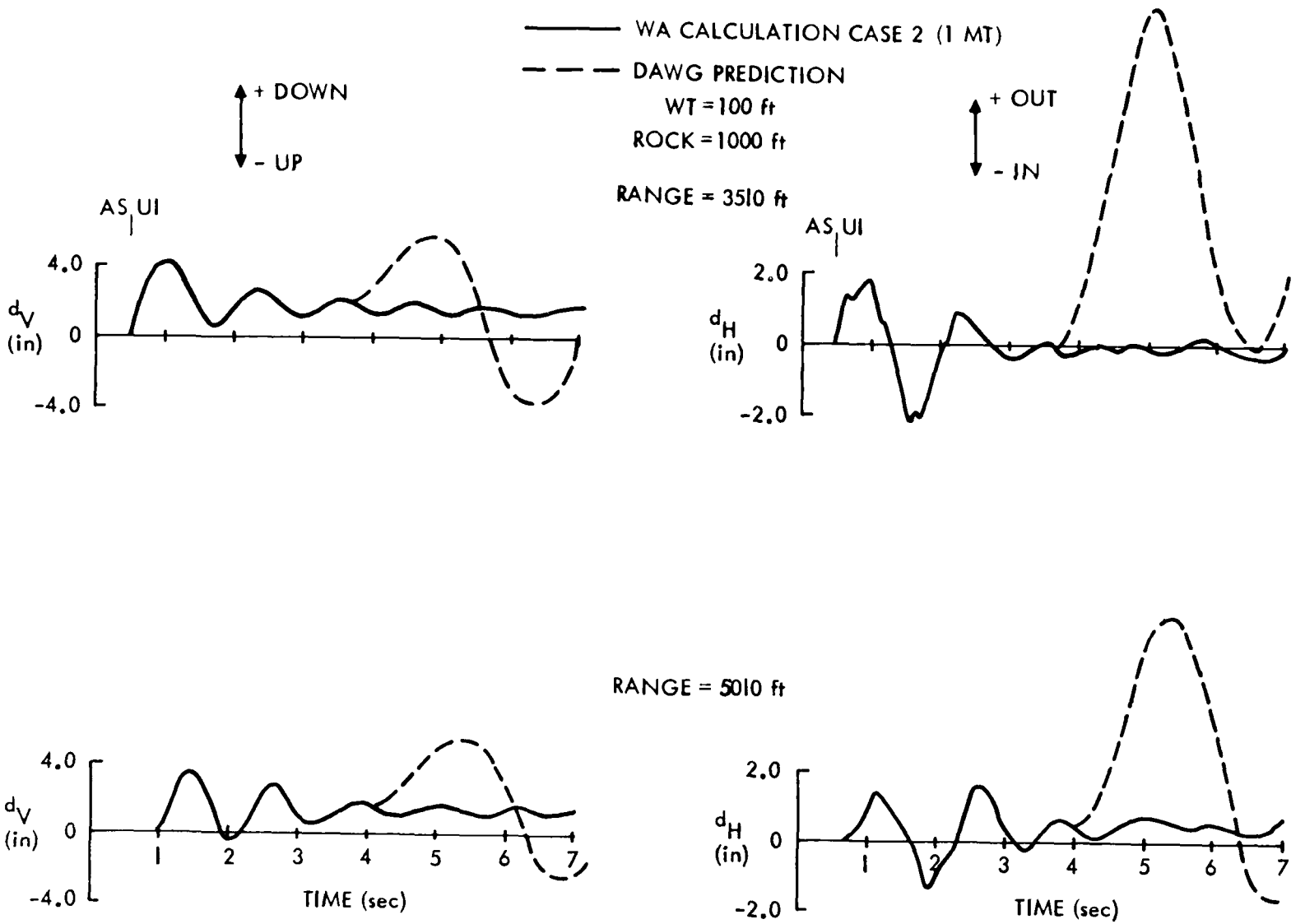

Figure 16. WA Calculation and DAWG Prediction Displacement Time History Comparison, Case 2, 3510 and 5010 ft Range

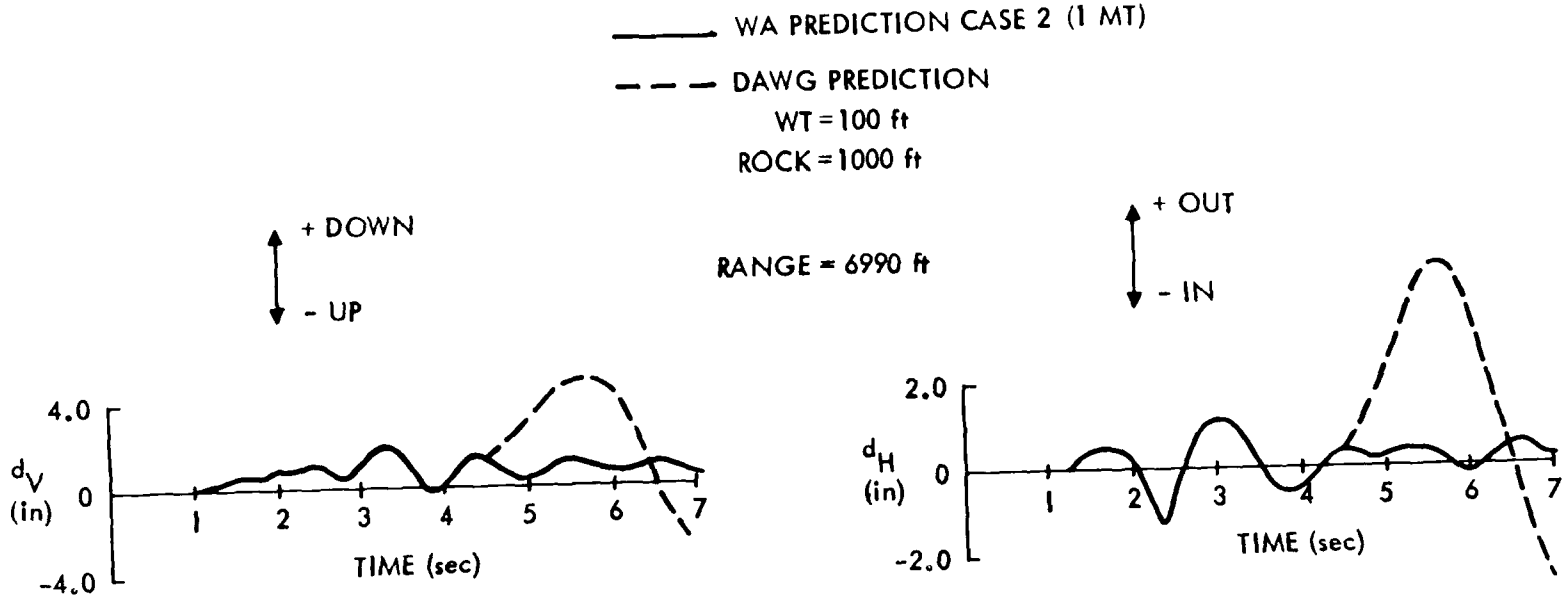

Figure 17. WA Calculation and DAWG Prediction Displacement Time History Comparison, Case 2, 6990 ft Range

modification to the DAWG waveform, currently being considered by Higgins, Auld and Associates, would divide the upstream-induced response into two components - one which propagates with S-Wave speeds and another which propagates with P-Wave speeds.

The DAWG peak velocity predictions are many times larger than WA calculation values for the higher overpressure ranges, while the oscillatory period is 2 or more times larger than that of the calculations, resulting in very large predicted upstream-induced displacements. Below 100 psi, the peak velocities of the DAWG predictions are much closer to those of the calculations. The oscillatory periods are still approximately a factor of 2 longer than in the calculations. Similar conclusions were obtained for the displacement comparisons at the larger ranges. These comparisons show peak displacement and frequency content to vary no more than a factor of 3 at the 6990 ft range.

Peak displacement comparisons are shown in Figure 18. Also included in the Figure are peak displacement predictions corresponding to (1) crater volume scaling (for surface burst crater volumes calculated using the Air Force Design Manual procedure) in the close-in region, and (2) analysis of NTS data [Cooper 1972] in the further-out region. The fact that the zero crater volume DAWG predictions show reasonable agreement with the crater volume scaling closer-in is purely accidental. It would be expected that the MX displacements be lower than the NTS line at long range because the NTS geology and yields correspond to a deeper scaled depth to rock. However, the DAWG predictions are higher. Additional parametric studies and analysis of existing calculations are required to better understand the behavior of the motions from finite element calculations and from the DAWG model and to explain any inconsistencies with the environments measured at NTS.

The 600 ft depth-to-rock calculations, Case 1, show a higher frequency of oscillation than for Case 2 (1000 ft to rock) which is reflected in the DAWG predictions. The initial motion of the vertical predictions is a small (compared to the peak value) signal downward rather than upward, as would be expected from a signal traveling within the deeper layers and then propagating up to the surface. The horizontal predictions have an initial motion outward which is as expected.

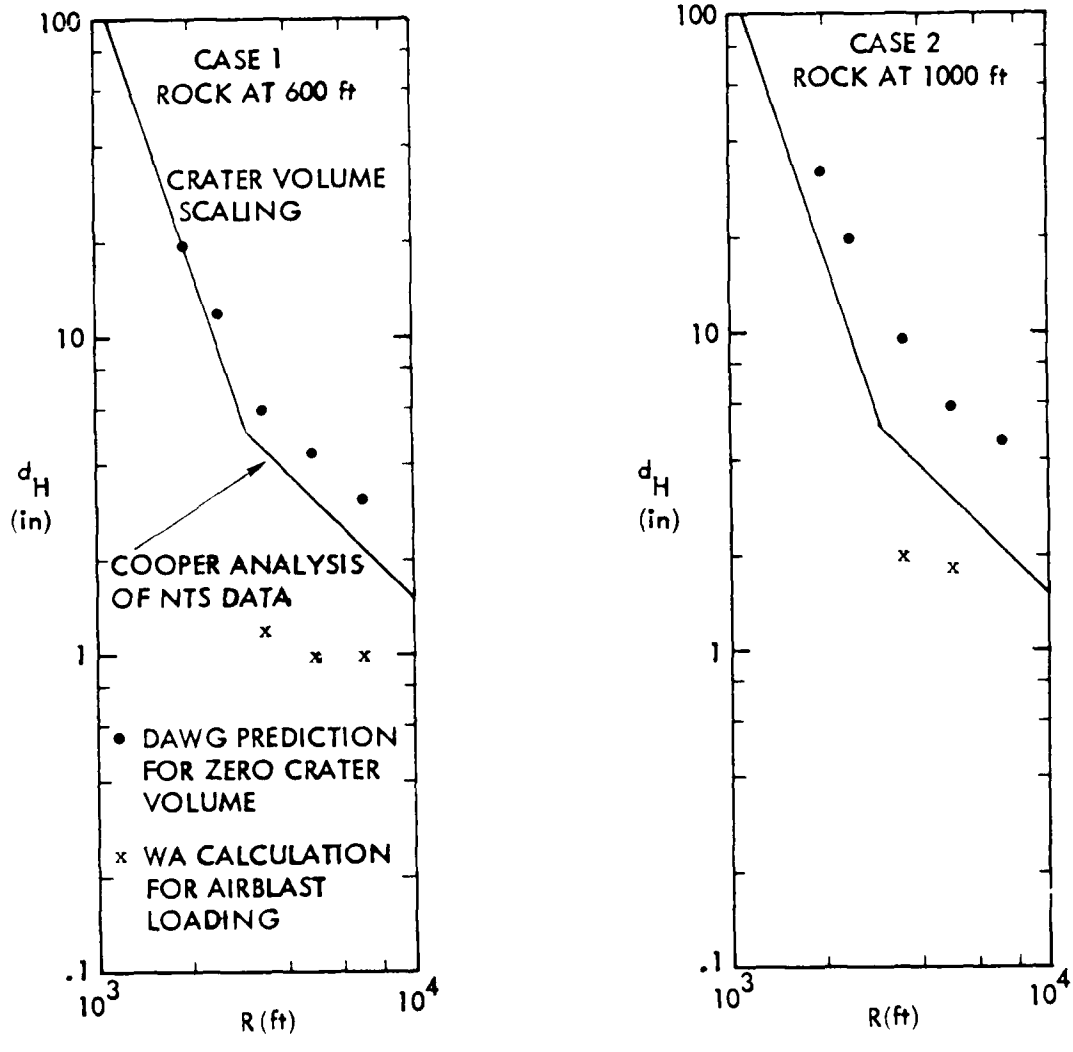

Figure 18. Horizontal Displacement Comparison (1 MT)

Free field velocity and displacement data for MIDDLE GUST III and IV are presented in Appendix B.

3.3 CLOSE-IN DISPLACEMENT PREDICTION

As previously discussed, crater-volume scaling is used for estimating the close-in ground motion displacements, based on analysis of results from nuclear and high explosive test events conducted before 1970. Data from such diverse geologies as hard rock (MINERAL ROCK and MINE ORE) and dry soil (e.g. PRAIRIE FLAT) were consistent with a single scaling law, although there was a large scatter in the data about the prediction.

A severe test of the scaling has been the PRE-DICE THROW II-1 and 2 120-T Ammonium Nitrate/Fuel Oil (100-ton TNT equivalent) surface-tangent events conducted in 1975 in a wet soil geology at White Sands, New Mexico. These events produced the largest craters for this yield and charge geometry; however, the displacements were not correspondingly larger. More recent analysis that includes these data show that, for geologies of interest to MX, the high explosive data are more consistent with yield scaling than with crater volume scaling. Regression analysis was performed on peak horizontal displacement data from most of the 100- and 500-ton surface-tangent high explosive events [Lipner 1978] with the results shown in Figure 19. Using crater volume scaling, the wet site (MIDDLE GUST III and PRE-DICE THROW II-1 and 2) events are systematically lower than the dry site events (PRAIRIE FLAT, DIAL PACK, DISTANT PLAIN 6, MIDDLE GUST IV, MIXED COMPANY 3, MINERAL ROCK, AND MINE ORE) by approximately a factor of 3. However, wet and dry site events are consistent with a geology-independent yield scaling for events in soil geologies with large depth to rock (PRAIRIE FLAT, DIAL PACK, DISTANT PLAIN 6, and PRE-DICE THROW II-1 and 2). As the depth to rock becomes shallower, the yield-scaled displacement decreases. Thus, the depth to rock appears to be more important than the depth to water table, while the reverse is generally true for crater volume scaling.

Scaling comparisons for nuclear data have also been performed [Lipner 1978]. These comparisons could not meaningfully distinguish between the two scaling procedures since the nuclear data base is too tenuous. Because of this and the fact that the high explosive events in rock are more consistent with crater volume scaling, the DAWG has not changed to yield scaling.

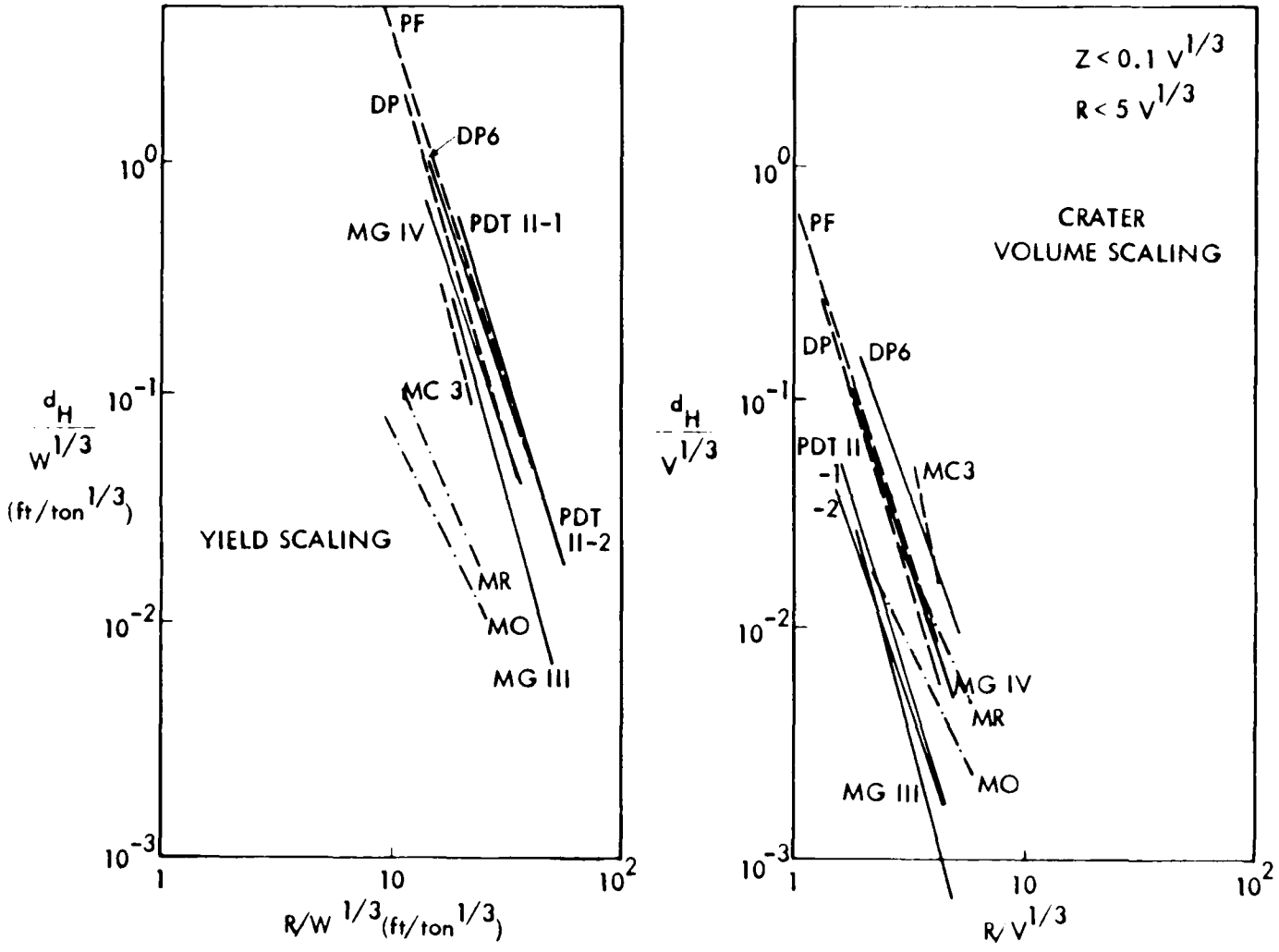

Figure 19. Surface Tangent High Explosive Peak Horizontal Displacement Scaling; 100 and 500 ton Events

However, the material behavior of rock media is different enough from soil media that the same scaling need not apply to both.

4.0 SUMMARY

The following is a summary of conclusions and recommendations regarding the upstream-induced ground motion component, based on the preliminary evaluation in this report:

(a) While the close-in high explosive horizontal velocity data have a relatively small geology sensitivity, there are systematic differences between results from events with shallow rock and with deep rock; horizontal velocities for shallow rock geologies being higher by an average factor of about 1.4, based on regression analysis results. However, the DAWG prediction is consistent with the data for geologies relevant to MX.

(b) The close-in high explosive vertical velocity data exhibit larger variation with geology than do the horizontal. The largest velocities appear to correspond to layered geologies with a large impedance mismatch. This may be associated with the fact that the head wave front propagating into the surface layer, for such a geology, has a shallow angle and, therefore, a large vertical component. Regression analysis of these data and further analysis of the phenomenology should also be performed.

(c) The factor of two energy equivalence used to relate high explosive peak velocities to nuclear predictions was not evaluated in this study. However, there are few nuclear data points on which such an equivalence can be based for the close-in region. This should be evaluated further in conjunction with DNA activities related to HE/NE equivalence issues.

(d) The plateau velocity in the DAWG prediction is directly a function of the depth to rock only. Geometric scaling considerations suggest that a yield-scaled depth to rock should be used. Finite difference computer code calculations should be performed to further evaluate this scaling.

(e) In the outrunning region, the MIDDLE GUST IV data are substantially larger (factor of 5 or greater) than the prediction. In this event, there was a late time, dominant high frequency response on the order of 5 Hz at some of the seismic stations. Plastic surface wave analysis should be performed to further investigate this response.

(f) The upstream-induced signals have arrival times corresponding to P-wave speeds in the DAWG prediction, while test data and finite element

calculations have initial upstream arrivals corresponding to P-Wave speeds. Furthermore, the predicted initial vertical motion is downward, while an initial upward upstream-induced response would be expected. A modification to the prediction to correct these problems is currently being developed by Higgins, Auld and Associates.

(g) Comparisons between WA finite element calculations and corresponding DAWG predictions show the DAWG displacements to be about a factor of 3 greater in the outrunning region, with an even larger difference close-in. Additional parametric analysis studies and analysis of existing calculations are required to better understand the DAWG model and to explain any differences with the environments measured at NTS.

(h) The high explosive data are more consistent with yield scaling than with crater volume scaling, for wet and dry soil geologies of interest to MX. The yield-scaled displacements, for the events analyzed, would appear to have a coefficient dependent on the depth to rock (and probably other parameters), but not on the depth to water table. DNA studies on HE/NE equivalence should address the issue of how to use the high explosive data base for prediction of close-in nuclear displacements.

(i) Other general recommendations are: (1) regression analyses are helpful in identifying event-to-event variations and DNA should support establishing a credible data base from which such analyses could be performed, (2) analysis of calculational results in a manner similar to that performed for test data is useful for determining the scaling implied by the calculations, and (3) performing calculational studies of high explosive events is about the best approach to developing predictions with reasonable confidence for a wide variety of geologies.

5.0 REFERENCES

1. Auld, H. E., and Murphy, J. R., *Surface Wave Simulations*, Proceedings, Defense Nuclear Agency Strategic Structures Division Biennial Review Conference held at Menlo Park, California, March 20-23, 1979.

2. Cooper, H. F., *Analysis of Burst Effects on Strong Motion Seismic Instruments from Nuclear Explosions*, RDA-TR-063-DNA, R&D Associates, Santa Monica, California, 29 April 1972.

3. Crawford, R. E., Higgins, C. J., and Bultman, E. H., *The Air Force Manual for Design and Analysis of Hardened Structures*, AFWL-TR-74-102, Air Force Weapons Laboratory, Kirtland Air Force Base, New Mexico, July 1974.

4. [Data Analysis Working Group], *Review of Parametric Nuclear Weapons Environment for MX Multiple Aimpoint Basing System Definition*, DAWG-TR-3, December 14, 1978.

5. Hadala, P. F., *Effect of the Constitutive Properties of Earth Media on Surface Ground Shock From Large Explosions*, TR S-73-6, U. S. Army Engineer Waterways Experiment Station, Vicksburg, Mississippi, August 1973.

6. Higgins, C. J. and Schreyer, H. L., *An Analysis of Cutrunning Ground Motions*, AFWL-TR-74-220, Air Force Weapons Laboratory, Kirtland Air Force Base, New Mexico, May 1975.

7. Jaramillo, E. E., *Middle Gust III Free Field Data Report*, AL-831-3, EG&G Inc., Albuquerque, New Mexico, 2 February 1973.

8. Joachim, C. E., *Empirical Predictions of Nuclear Explosion Ground Motions in the Cutrunning Region*, U.S. Army Engineer Waterways Experiment Station, Vicksburg, Mississippi, December 1973.

9. Lipner, N., Anderson, D. C., and Dai, P. K., *Ground Motion Environments for Generic Site Conditions*, DNA-3872F, Defense Nuclear Agency, Washington, DC, December 1975.

10. Lipner, N., "Crater-Related Horizontal Displacement Scaling," Minutes of the Fourteenth Meeting of the Data Analysis Working Group at Albuquerque on November 1978. General Electric Company - TEMPO, Albuquerque, New Mexico.

11. Murphy, J. R. and Bennett, T. J., *Analysis of the Low Frequency Ground Motion Environment for MX: Surface Wave and Valley Reverberation - Theory*, SSS-R-80-4298, Systems, Science and Software, Reston, Virginia, January 1980; to be issued as DNA-5210F, Defense Nuclear Agency, Washington, DC.

5.0 REFERENCES (continued)

12. [MX NWE V-4 Working Group], *Multiple Buried Inert Nuke Earth Motions, Interim Report on MX NWE Test V-4 - Buried Array*, Air Force Weapons Laboratory, Kirtland Air Force Base, New Mexico, January 10, 1980.

13. Pozega, R. E., *Middle East II Free Field Data Report*, AL-831-4, EG&E Inc., Albuquerque, New Mexico, 1 May 1973.

14. Sandler, I. S., *Improving Buried Motion Simulations Data Package for Near Analysis Working Group*, Weidlinger Associates, New York, November 1978. (Unpublished)

15. Sauer, F. M., Clark, G. B., and Anderson, D. C., "Empirical Analysis of Ground Motion and Cratering, Part IV," *Nuclear Geophysics*, DASA-1285 (IV), Defense Atomic Support Agency, Washington, DC, May 1964.

16. [Weidlinger] *Progress Report No. 7*, Contract No. DNA001-77-C-0036, Weidlinger Associates, New York, May 1977.

APPENDIX A

DAWG PREDICTION WAVEFORM EQUATIONS

The DAWG prediction waveform is presented in the following equations along with input requirements.

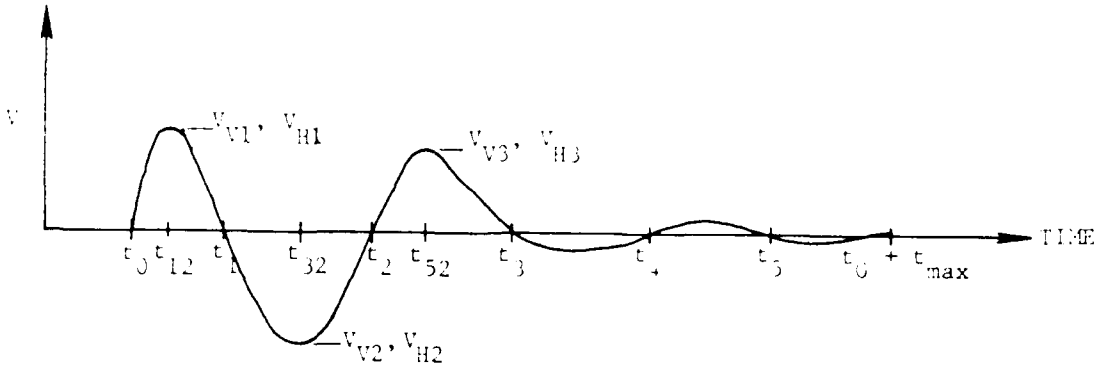

INPUT REQUIREMENTS:

W' = Yield

R = Range

H = Depth to Rock

C_{S_1} = Average Shear Wave Speed Above Rock

C_{S_2} = Shear Wave Speed of Rock

CRAVTOL = Crater Volume

V_{LF} = Peak Velocity (from Figure 3)

WAVEFORM EQUATIONS

VERTICAL

For $t < t_{52V}$

$$V_V = V_{OV} t \exp^{(T_{DV})} \text{SIN}\theta_V$$

$$\gamma_V = \begin{cases} \dfrac{t}{E_V + F_V t} & \text{for } t \leq t_{2V} \\ \gamma_V(t - t_{2V}) & \text{for } t > t_{2V} \end{cases}$$

$$T_{DV} = \begin{cases} D_V(t_{12V} - t) & \text{for } t \leq t_{32V} \\ D_V(t_{12V} - t) + D_{2V}(t_{32V} - t) \cdot \\ \text{SIN}[G_{2V}(t - t_{32V})] & \text{for } t > t_{32V} \end{cases}$$

For $t \geq t_{52V}$

$$V_V = V_{V3} \exp\left[\frac{t_{52V} - t}{t_{DECAY}}\right] \text{SIN}[\gamma_V(t - t_{2V})]$$

HORIZONTAL

For $t < t_{52H}$

$$V_H = V_{OH} t \exp^{(T_{DH})} \text{SIN}\theta_H$$

$$\gamma_H = \begin{cases} \dfrac{t}{E_H + F_H t} & \text{for } t \leq t_{2H} \\ \gamma_H(t - t_{2H}) & \text{for } t > t_{2H} \end{cases}$$

$$D_{DH} = \begin{cases} D_H(t_{12H} - t) & \text{for } t \leq t_{32H} \\ D_H(t_{12H} - t) + D_{2H}(t_{32H} - t) \cdot \\ \text{SIN}[G_{2H}(t - t_{32H})] & \text{for } t > t_{32H} \end{cases}$$

For $t \geq t_{52H}$

$$V_H = V_{H3} \exp\left[\frac{t_{52H} - t}{t_{DECAY}}\right] \text{SIN}[\gamma_H(t - t_{2H})]$$

PEAK VELOCITIES

$$V_{V1} = \frac{\overline{V}_{V1}}{\overline{V}_{V2}} V_{LF}$$

$$V_{V2} = V_{LF}$$

$$V_{V3} = \frac{\overline{V}_{V3}}{\overline{V}_{V2}} V_{LF}$$

IF $\overline{V}_{H1} > \overline{V}_{H2}$

$$V_{H1} = V_{LF}$$

$$V_{H2} = \frac{\overline{V}_{H2}}{\overline{V}_{H1}} V_{LF}$$

$$V_{H3} = \frac{\overline{V}_{H3}}{\overline{V}_{H1}} V_{LF}$$

IF $V_{H2} > V_{H1}$

$$V_{H1} = \frac{\bar{V}_{H1}}{\bar{V}_{H2}} V_{LF}$$

$$V_{H2} = V_{LF}$$

$$V_{H3} = \frac{\bar{V}_{H3}}{\bar{V}_{H2}} V_{LF}$$

$$\bar{V}_{V1} = \text{minimum of} \begin{cases} \text{maximum of} \begin{cases} \dfrac{-0.54}{(R/W^{1/3})^{0.66}} \\ -0.5\bar{V}_{V2} \end{cases} \\ -0.2\bar{V}_{V2} \end{cases}$$

$$\bar{V}_{H1} = \text{maximum of} \begin{cases} \dfrac{12.0}{(R/W^{1/3})^{2.3}} \\ \dfrac{\bar{V}_{H2}}{2.0} \end{cases}$$

$$\bar{V}_{V2} = \text{maximum of} \begin{cases} \dfrac{1.9}{(R/W^{1/3})^{1.2}} \\ \dfrac{16.0}{(R/W^{1/3})^{2.7}} \end{cases}$$

$$\bar{V}_{H2} = \frac{3.6}{(R/W^{1/3})^{1.4}}$$

$$\bar{V}_{V3} = \begin{cases} \text{maximum of} \begin{cases} \dfrac{-7.4}{(R/W^{1/3})^{2.0}} \\ -0.9\bar{V}_{V2} \end{cases} & \text{for } (R/W^{1/3}) \leq 3 \\ -0.9\bar{V}_{V2} & \text{for } (R/W^{1/3}) \leq 3 \end{cases}$$

$$\bar{V}_{H3} = \text{minimum of} \begin{cases} \dfrac{1.5}{(R/W^{1/3})^{0.8}} \\ 0.9V_{H2} \end{cases}$$

TIME VALUES

$$T = \frac{2.0\ H}{C_{S1}}$$

$$t_O = t_{OGR} + t_{DECAY}$$

$$t_{OGR} = \text{minimum of} \begin{cases} \dfrac{R}{C_{S2}} + 2H\sqrt{\left(\dfrac{1}{C_{S1}}\right)^2 - \left(\dfrac{1}{C_{S2}}\right)^2} \\ \dfrac{R}{C_{S1}} \end{cases}$$

$$t_{1V} = \text{maximum of} \begin{cases} \text{minimum of} \begin{cases} 0.25(R/W^{1/3})\dfrac{T}{2} \\ \dfrac{T}{2} \end{cases} \\ 0.13\ t_{2H}^{*} \end{cases}$$

$$t_{1H} = \text{maximum of} \begin{cases} \dfrac{\pi d_H}{2V_{LF}} \cdot \dfrac{1000\ \text{msec}}{\text{sec}} \\ \dfrac{T}{2} \end{cases}$$

$$t_{2V} = t_{1V} + t_{1H}$$

$$t_{2H} = \text{maximum of} \begin{cases} \left[3 - \dfrac{(R/W^{1/3})}{3}\right] t_{1H} \\ 2t_{1H} \end{cases}$$

* First value calculated for t_{1H}

The peak horizontal displacement must be within 5% of the value d_H. If this requirement is not satisfied, modify t_{1H} and t_{2H} as follows, and recalculate a new velocity time history.

$$t_{1H} = \text{maximum of} \begin{cases} \dfrac{T}{2} \\ t_{1H}\dfrac{d_H}{d_{HCALC}} \end{cases}$$

where d_{HCALC} = maximum horizontal displacement from previous iteration

$$t_{2H} = \text{maximum of} \begin{cases} \left[3 - \dfrac{(R/W^{1/3})}{3}\right] t_{1H} \\ 2t_{1H} \end{cases}$$

EQUATION CONSTANTS

$$d_H = \frac{0.45(\text{CRATVOL})^{4/3}}{R^3}$$

$$t_{DECAY} = \begin{cases} T & \text{for } (R/W^{1/3}) \leq 5 \\ 0.2(R/W^{1/3})T & \text{for } 5 \leq (R/W^{1/3}) \leq 15 \\ (3.0)T & \text{for } (R/W^{1/3}) > 15 \end{cases}$$

$$E_V = \frac{t_{1V}\, t_{2V}}{2\pi(t_{2V} - t_{1V})} \qquad E_H = \frac{t_{1H}\, t_{2H}}{2\pi(t_{2H} - t_{1H})}$$

$$F_V = \frac{.5t_{2V} - t_{1V}}{\pi(t_{2V} - t_{1V})} \qquad F_H = \frac{.5t_{2H} - t_{1H}}{\pi(t_{2H} - t_{1H})}$$

$$\gamma_V = \frac{\pi}{t_{2V} - t_{1V}} \qquad \gamma_H = \frac{\pi}{t_{2H} - t_{1H}}$$

$$t_{12V} = \frac{\pi E_V}{2 - \pi F_V} \qquad t_{12H} = \frac{\pi E_H}{2 - \pi F_H}$$

$$t_{32V} = \frac{3\pi E_V}{2 - 3\pi F_V} \qquad t_{32H} = \frac{3\pi E_H}{2 - 3\pi F_H}$$

$$t_{52V} = t_{2V} + \frac{\pi}{2\gamma_V} \qquad t_{52H} = t_{2H} + \frac{\pi}{2\gamma_H}$$

$$V_{OV} = \frac{V_{V1}}{t_{12V}} \qquad V_{OH} = \frac{V_{H1}}{t_{12H}}$$

$$D_V = \frac{LN\left(-\frac{V_{OV}}{V_{V2}}\, t_{32V}\right)}{t_{32V} - t_{12V}} \qquad D_H = \frac{LN\left(\frac{V_{OH}}{V_{H2}}\, t_{32H}\right)}{t_{32H} - t_{12H}}$$

$$G_{2V} = \frac{\pi}{2} \frac{1}{(t_{52V} - t_{32V})} \qquad G_{2H} = \frac{\pi}{2} \frac{1}{(t_{52H} - t_{32H})}$$

$$D_{2V} = \frac{LN\left(\frac{V_{V3}}{V_{OV}\ t_{52V}}\right) + D_V(t_{52V} - t_{12V})}{t_{32V} - t_{52V}} \qquad D_{2H} = \frac{LN\left(\frac{V_{H3}}{V_{OH}\ t_{52H}}\right) + D_H(t_{52H} - t_{12H})}{t_{32H} - t_{52H}}$$

$$t_{max} = 2t_{2H} - t_{1H} + 4t_{DECAY}$$

$$W(LB_{HE}) = \frac{W'(kT_N) \cdot 2 \times 10^6 (LB_N)}{\frac{2(LB_N)}{(LB_{HE})}}$$

APPENDIX B

MIDDLE GUST III AND IV DATA

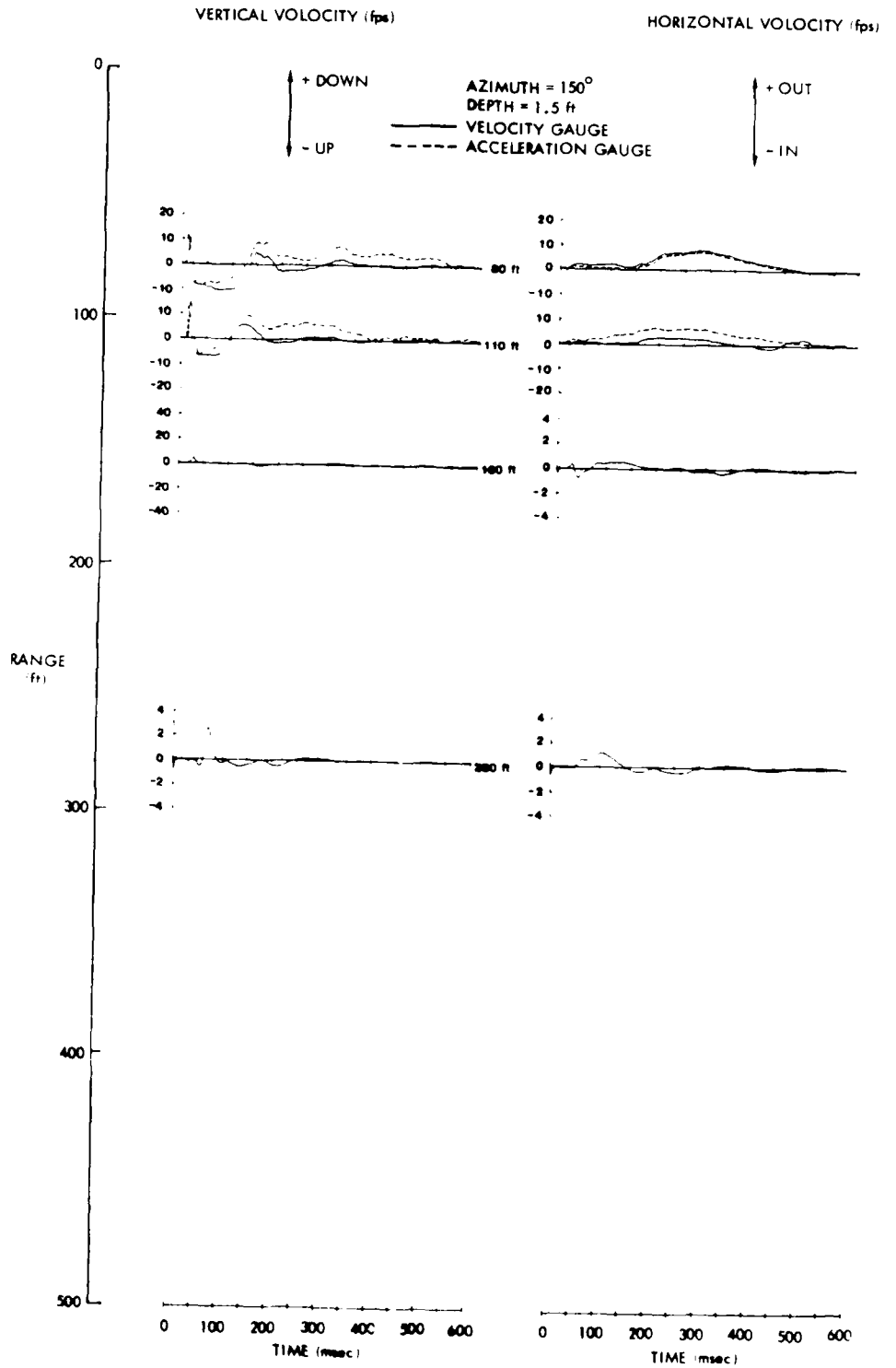

Figure B1. Middle Gust III Velocity Time History Data, 150°, 1.5 ft Depth

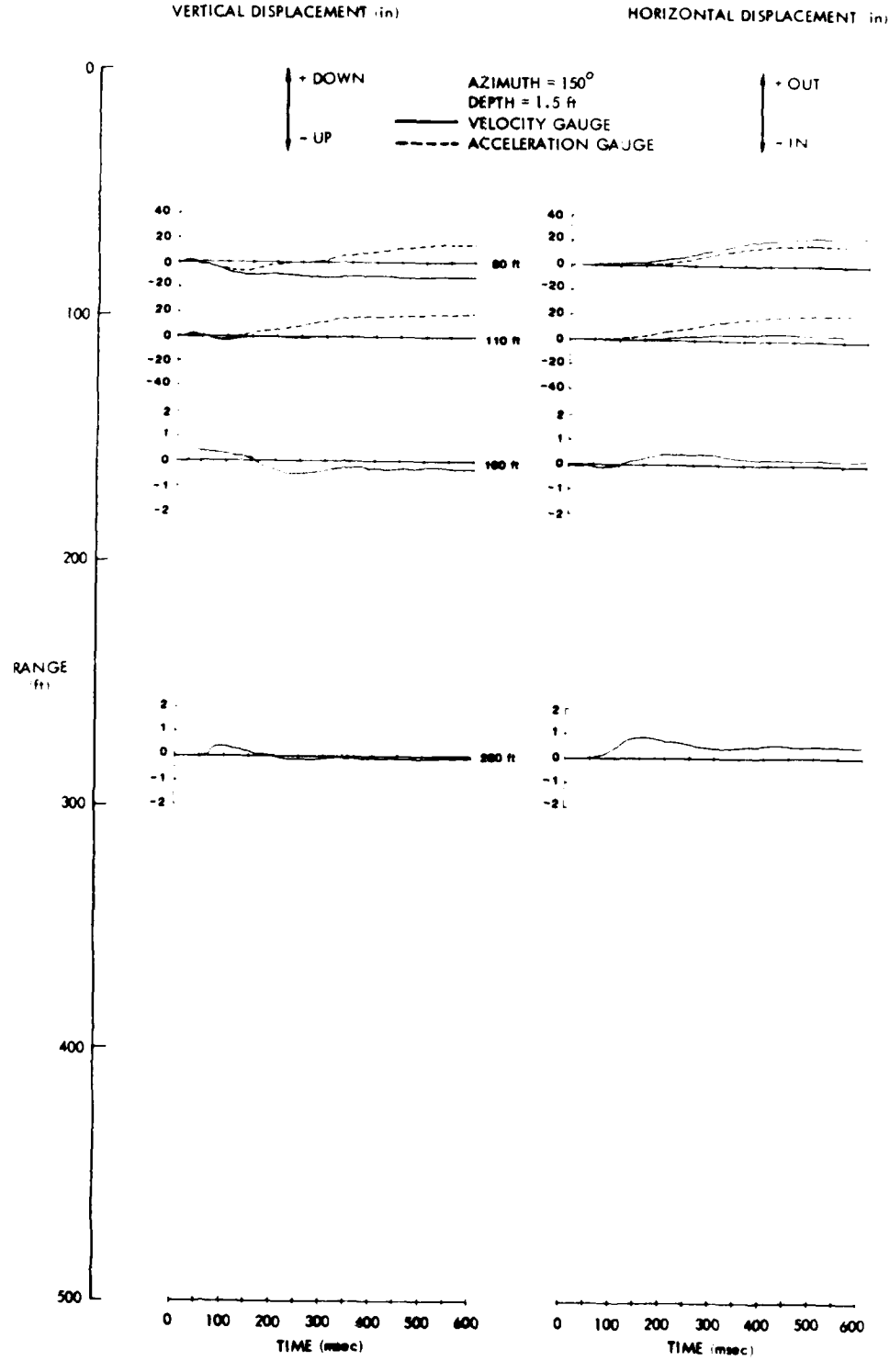

Figure B2. Middle Gust III Displacement Time History Data, 150°, 1.5 ft Depth

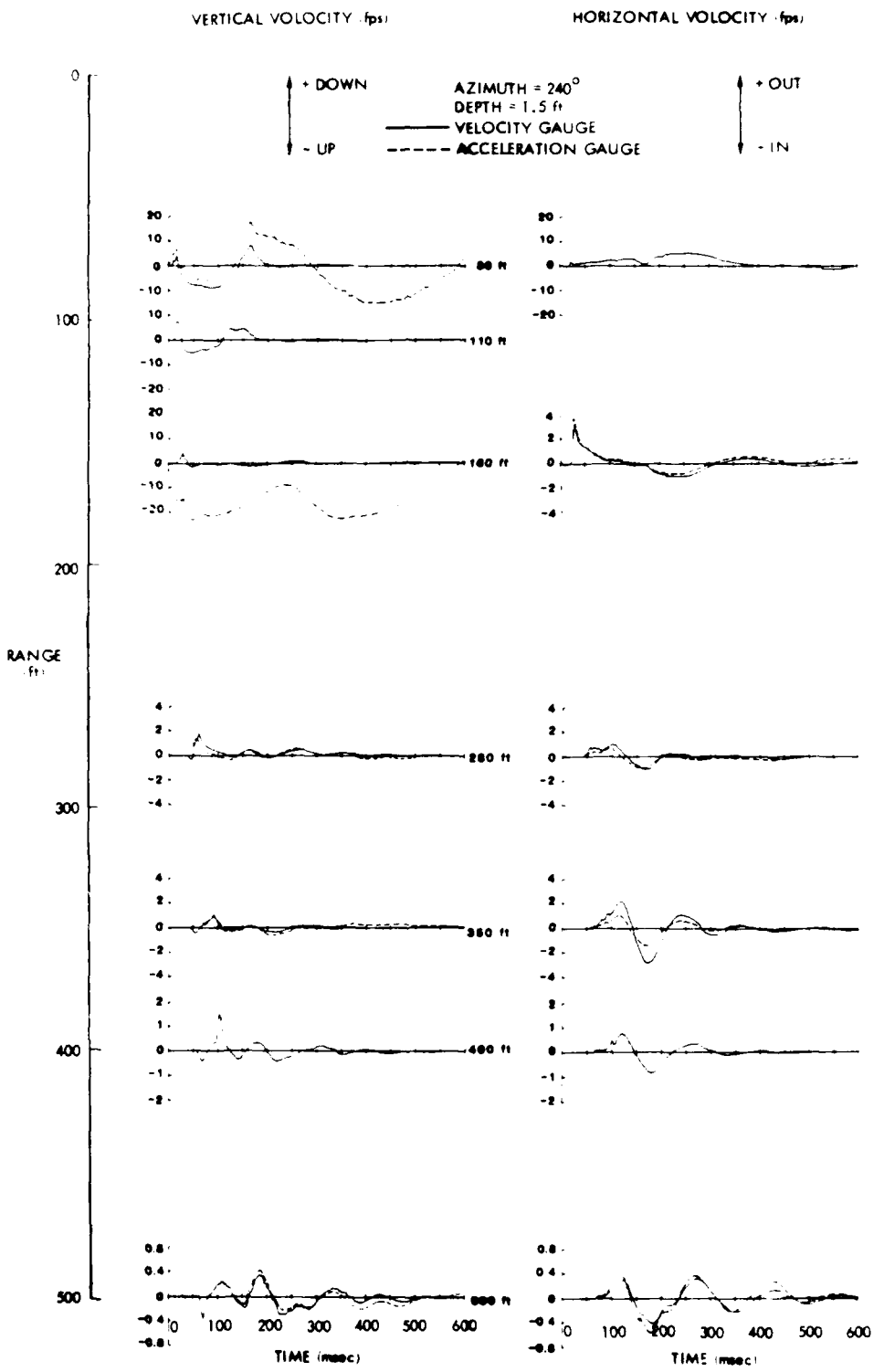

Figure B3. Middle Gust III Velocity Time History Data, 240°, 1.5 ft Depth

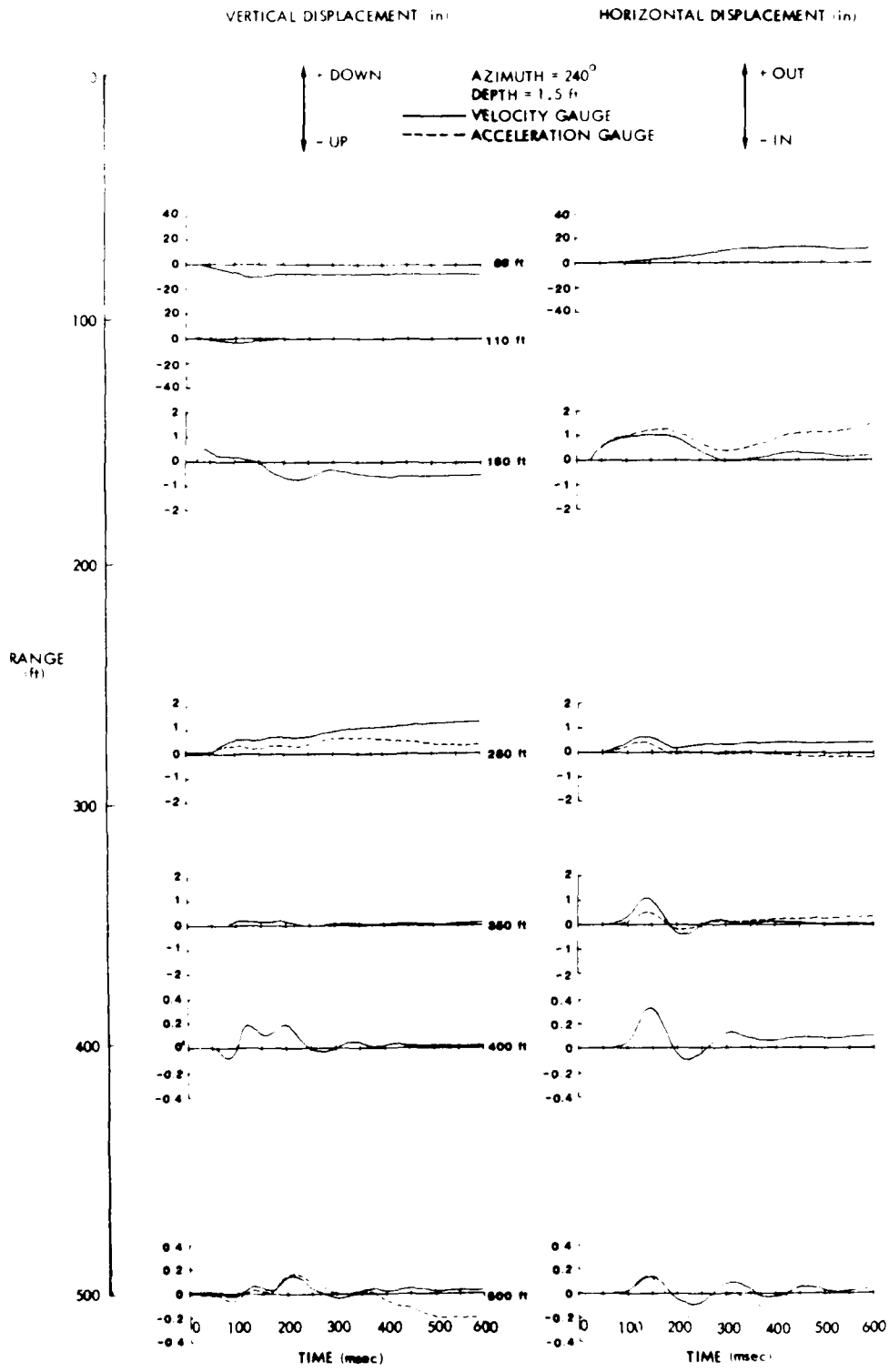

Figure B4. Middle Gust III Displacement Time History Data, 240°, 1.5 ft Depth

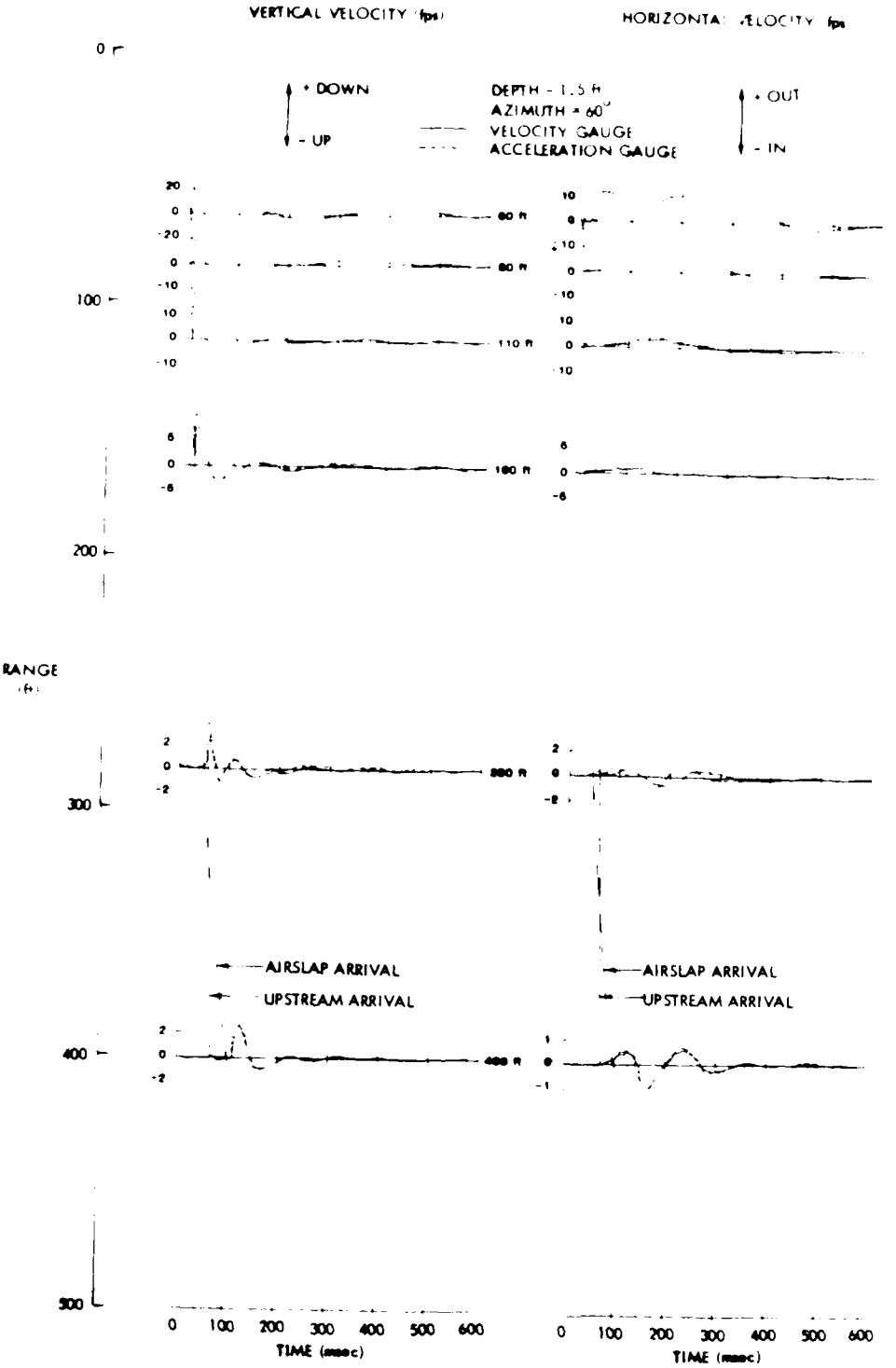

Figure B5. Middle Gust IV Velocity Time History Data, 60°, 1.5 ft Depth

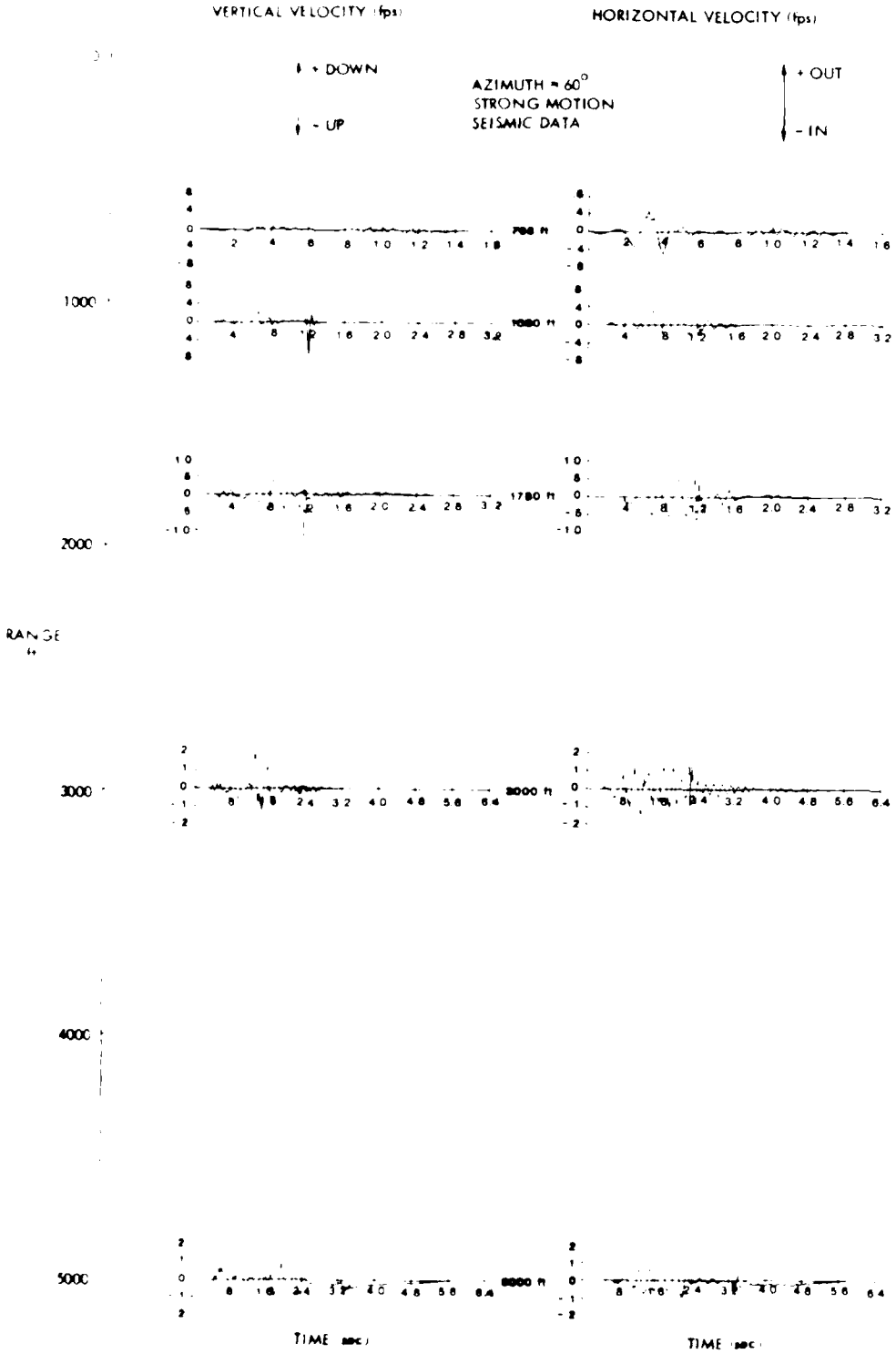

Figure 36. Middle Gust IV Strong Motion Seismic Velocity Time History Data, 60°

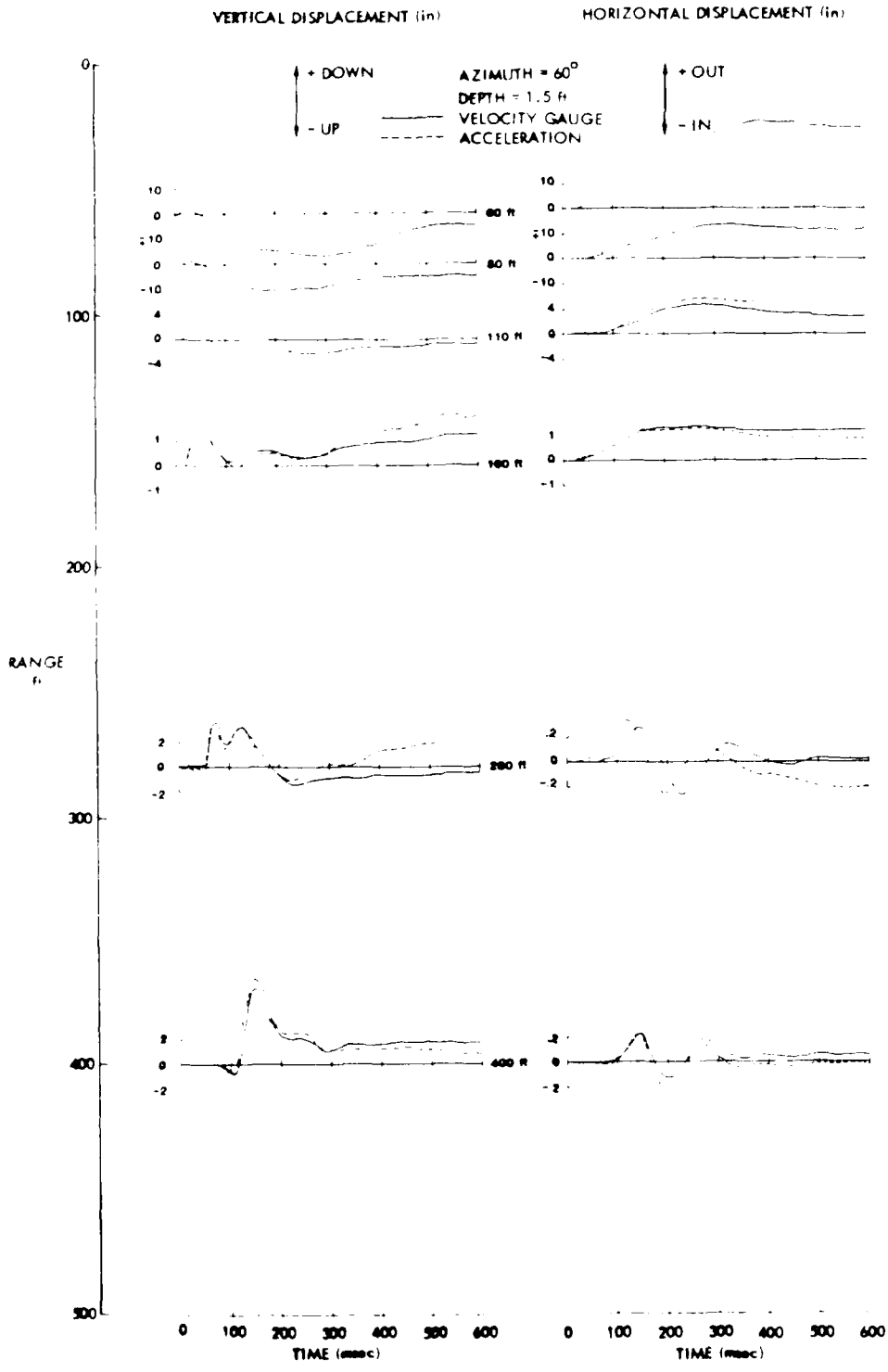

Figure B7. Middle Gust IV Displacement Time History Data, 60°, 1.5 ft Depth

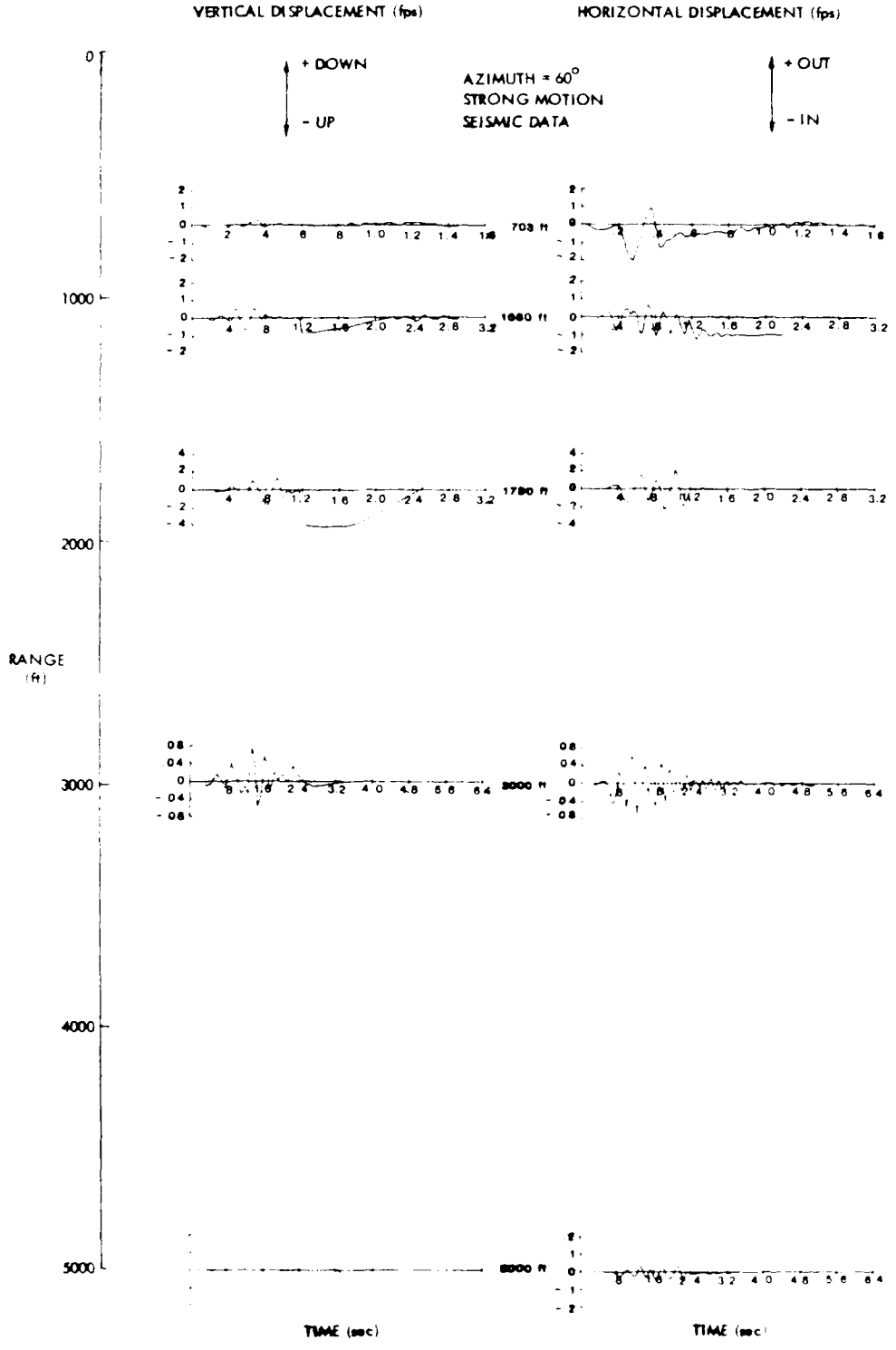

Figure B8. Middle Gust IV Strong Motion Seismic Displacement Time History Data, 60°

DISTRIBUTION LIST

DEPARTMENT OF THE AIR FORCE (Continued)

Assistant Chief of Staff
Intelligence
Department of the Air Force
ATTN: IN

Assistant Secretary of the Air Force
Research, Development & Logistics
ATTN: SAFALR/DEP for Strat & Space Sys

Ballistic Missile Office
Air Force Systems Command
ATTN: MNNX, W. Crabtree
ATTN: MNNXH, M. Delvecchio
ATTN: MNNXH, D. Gage

Strategic Air Command
Department of the Air Force
ATTN: J. McKinney

Deputy Chief of Staff
Research, Development, & Acq
Department of the Air Force
ATTN: AFRDQI, N. Alexandrow
ATTN: AFRDPN
ATTN: AFRDQA
ATTN: AFRDQI

Strategic Air Command
Department of the Air Force
ATTN: XPFS
ATTN: NRI-STINFO Library

VELA Seismology Center
Department of the Air Force
ATTN: G. Ullrich

OTHER GOVERNMENT AGENCY

Central Intelligence Agency
ATTN: OSWR/NED

DEPARTMENT OF ENERGY CONTRACTORS

Lawrence Livermore National Laboratory
ATTN: D. Glenn

Los Alamos National Scientific Laboratory
ATTN: R. Sanford
ATTN: C. Keller

Sandia National Laboratories
ATTN: A. Chabai
ATTN: Org 1250, W. Brown

DEPARTMENT OF DEFENSE CONTRACTORS

Acurex Corp
ATTN: J. Stockton
ATTN: K. Triebes
ATTN: C. Wolf

Aerospace Corp
ATTN: H. Mirels
ATTN: Technical Information Services

Agbabian Associates
ATTN: M. Agbabian

DEPARTMENT OF DEFENSE CONTRACTORS (Continued)

Applied Theory, Inc
2 cy ATTN: J. Trulio

Artec Associates, Inc
ATTN: S. Gill

Boeing Co
ATTN: Aerospace Library
ATTN: S. Strack

California Research & Technology, Inc
ATTN: M. Rosenblatt
ATTN: Library

University of Denver
ATTN: J. Wisotski

Eric H. Wang
Civil Engineering Rsch Fac
University of New Mexico
ATTN: J. Kovarna
ATTN: P. Lodde
ATTN: J. Lamb

General Electric Company—TEMPO
ATTN: DASIAC

H-Tech Labs, Inc
ATTN: B. Hartenbaum

Higgins, Auld & Associates
ATTN: J. Bratton
ATTN: N. Higgins
ATTN: H. Auld

IIT Research Institute
ATTN: Documents Library

J. H. Wiggins Co, Inc
ATTN: J. Collins

Kaman AviDyne
ATTN: R. Ruetenik

Merritt CASES, Inc
ATTN: Library

Mission Research Corp
ATTN: G. McCartor
ATTN: C. Longmire

Nathan M. Newmark Consult Eng Svcs
ATTN: N. Newmark
ATTN: W. Hall

Pacific-Sierra Research Corp
ATTN: H. Brode

Pacifica Technology
ATTN: Tech Library

Physics International Co
ATTN: J. Thomsen
ATTN: Technical Library
ATTN: F. Sauer

DEPARTMENT OF DEFENSE CONTRACTORS (Continued)

R & D Associates
ATTN: R. Port
ATTN: J. Carpenter
ATTN: A. Kuhl
ATTN: J. Lewis
ATTN: Technical Information Center
ATTN: P. Haas

Science Applications, Inc
ATTN: R. Schlaug
ATTN: H. Wilson
ATTN: Technical Library

Science Applications, Inc
ATTN: D. Hove

Science Applications, Inc
ATTN: B. Chambers III
ATTN: W. Layson

SRI International
ATTN: J. Colton
ATTN: D. Johnson
ATTN: G. Abrahamson
ATTN: Library

Systems, Science & Software, Inc
ATTN: C. Needham

Systems, Science & Software, Inc
ATTN: J. Murphy

DEPARTMENT OF DEFENSE CONTRACTORS (Continued)

Systems, Science & Software, Inc
ATTN: K. Pyatt
ATTN: J. Barthel
ATTN: Library

Systems, Science & Software, Inc
ATTN: C. Hastings

Terra Tek, Inc
ATTN: A. Abou-Sayed
ATTN: Library

TRW Defense & Space Sys Group
ATTN: Technical Info Center
ATTN: N. Lipner
ATTN: T. Mazzola

TRW Defense & Space Sys Group
ATTN: P. Dai
ATTN: E. Wong
ATTN: G. Hulcher

Weidlinger Assoc, Consulting Engineers
ATTN: I. Sandler

Weidlinger Assoc, Consulting Engineers
ATTN: J. Isenberg

END

DATE
FILMED

5 81

DTIC